

UNIVERZA V LJUBLJANI  
FAKULTETA ZA FARMACIJO

JAN BREZNIKAR  
MAGISTRSKA NAOGA  
ENOVITI MAGISTRSKI ŠTUDIJ FARMACIJE

Ljubljana, 2017

UNIVERSITY OF LJUBLJANA

FACULTY OF PHARMACY

JAN BREZNIKAR

**FORMATION AND STABILITY OF EYE DROPS CONTAINING  
CYCLOSPORINE ENCAPSULATED INTO QUATERNARY AMMONIUM  
PALMITOYL GLYCOL CHITOSAN NANOPARTICLES**

**IZDELAVA IN STABILNOST KAPLJIC ZA OČI S CIKLOSPORINOM,  
VGRAJENIM V NANODELCE KVARTERNEGA AMONIJEVEGA PALMITOIL  
GLIKOL HITOSANA**

Ljubljana, 2017

Magistško nalogo sem opravil na Fakulteti za farmacijo pod mentorstvom izr. prof. dr. Matjaža Jerasa in somentorstvom prof. dr. Ijome Uchegbu.

Izdelavo formulacije, kromatografske metode, preizkus sterilnosti in ostale meritve sem opravil na School of Pharmacy, University College London, Združeno kraljestvo Velike Britanije in Severne Irske.

### **Zahvala**

Ob tej priložnosti bi se rad iskreno zahvalil mentorju prof.dr. Matjažu Jerasu, ki me je vodil in mi s strokovnimi nasveti pomagal pri izdelavi magistrske naloge. Velika zahvala gre somentorici prof. dr. Ijomi Uchegbu, ki mi je dala priložnost, da eksperimentalni del opravim na School of Pharmacy, University College London, me vzpodbujala in usmerjala pri delu v laboratoriju. Najlepša hvala dr. Davidu Workmanu, dr. Nicku Hobsonu, dr. Xian Weng Jiangu, dr. Ramesh Soundararajanu, Isabel Gonçaves in vsem iz delovne skupine prof. dr. Ijome Uchegbum, ki so me veliko naučili in mi pomagali pri delu v laboratoriju. Hvala tudi dr. Paulu Stapletonuu, Sarah Soares in Pedru Ernesto de Resende, ki so me naučili dela z bakterijami. Hvala tudi predsedniku komisije prof. dr. Janko Kosu in članu komisije prof. dr. Roku Dreu, ki sta si vzela čas, pregledala in ocenila nalogo. Zahvaljujem se tudi družini, najbližnjim in prijateljem za vse lepe trenutke in vzpodbudne besede tekom študija.

### **Acknowledgment**

I would like to give my special thanks to Prof. dr. Matjaž Jeras, who with knowledge and advices leaded me through whole process of making the thesis. My deepest gratitude goes to Prof. Dr. Ijemoa Uchegbu, who gave me an opportunity to work in her group at School of Pharmacy, University College London, and encourageed me and leaded me through experimental work. I am particularly grateful for the assistance of Dr. David Workman, Dr. Nick Hobson, Dr Xian Weng Jiangu, Dr. Ramesh Soundararajanu, Isabel Gonçaves, and all working group who share their knowledge and helped me at laboratory work. Additionally, my thanks goes to Dr. Paul Stapleton, Sarah Soares and Perdo Ernsto de Resende, who helped me handling bacteria. I would also like to thank the commission board, president Prof. Dr Janko Kos, member and Prof. Dr Rok Dreu, who spent time to read and evaluate the thesis. One big thank also to my family, closest friends and colleges for all the nice memories and encouraging word during my student years.

## **Izjava**

Izjavljam, da sem magistrsko nalogo samostojno izdelal pod mentorstvom izr.prof. dr. Matjaža Jerasa in somentorstvom prof. dr. Ijome Uchegbu.

Jan Breznikar

Ljubljana, 2017

Predsednik komisije: Prof. dr. Janko Kos, mag. farm.

Član komisije: Izr. prof. dr. Rok Dreu, mag. farm.

## Table of content

Table of figures.....	iv
ABSTRACT .....	viii
POVZETEK .....	ix
LIST OF ABBREVIATIONS .....	xi
1. INTRODUCTION.....	1
1.1. Eyes.....	1
1.2. Eye diseases and epidemiology .....	2
1.3. Formulations for treatment of eye diseases .....	4
1.4. Formation of nanoparticles (homogenization).....	5
1.5. Quaternary Ammonium Palmitoyl Glycol Chitosan (GCPQ) .....	6
1.6. Cyclosporine A (CsA) .....	7
1.7. Characterization of formulations .....	8
1.7.1. Dynamic Light Scattering (DLS) .....	8
1.7.2. Zeta potential .....	9
1.7.3. Osmolarity .....	9
1.7.4. Viscosity .....	10
1.7.5. Evaporative light scattering detection (ELSD).....	11
2. AIMS AND OBJECTIVES .....	12
3. MATERIALS AND METHODS .....	13
3.1. Materials: .....	13
3.2. Solvents:.....	13
3.3. Reagents:.....	13
3.5. Synthesis of GCPQ .....	15
3.5.1. Degradation of glycol chitosan (GC).....	15

3.5.1. Palmitoylation of degraded glycol chitosan (dGC) to N-palmitoyl glycol chitosan (pGC).....	16
3.5.2. Quaternization of pGC.....	18
3.5.3. Iodine removal.....	20
3.6. Characterization of GCPQ.....	20
3.6.1. NMR analysis.....	20
3.6.2. GCP MALLS analysis.....	21
3.7. Calibration curve for CsA.....	22
3.7.1. HPLC analysis of CsA.....	22
3.8. Improving solubility of CsA before homogenization to achieve its higher encapsulation yields.....	23
3.9. Reducing the number of homogenization cycles.....	23
3.10. Production of eye drops.....	24
3.10.1. High pressure homogenization.....	24
3.10.2. pH value adjustment.....	25
3.11. Stability test.....	25
3.11.1. CsA concentration.....	26
3.11.2. Osmolarity.....	26
3.11.3. Viscosity.....	26
3.11.4. Zeta potential and particle size.....	26
3.12. The GCPQ assay.....	26
3.13. Sterility test.....	27
4. RESULTS AND DISCUSSION.....	29
4.1. Synthesis of GCPQ.....	29
4.1.1. GCPQ NMR analysis.....	30
4.2. CsA calibration curve.....	31
4.3. Quantification of CsA with HPLC.....	31

4.4. Improving the solubility of CsA before homogenization to achieve its higher encapsulation yields .....	34
4.5. Reduction of the number of homogenization cycles .....	35
4.6. Formulation stability .....	39
4.6.1. The GCPQ concentration assay .....	39
4.6.2. Concentrations of CsA .....	42
4.6.3. Osmolarity .....	43
4.6.4. Viscosity .....	45
4.6.5. Zeta potential .....	47
4.6.6. Particle size.....	48
4.7. Sterility test, according to USP 39 .....	56
4.7.1. Growth promotion test.....	57
4.7.2. Method suitability test .....	58
4.7.3. Sterility test.....	59
4.7.4. Plates.....	60
5. Conclusion .....	62
6. Literature .....	63

## Table of figures

Figure 1: Schematic presentation of an HPH cell.....	6
Figure 2: The chemical structure of GCPQ.....	7
Figure 3: Chemical structure of Cyclosporine A (25). ....	8
Figure 4: Graph, representing the principles of freezing point depression technique.....	10
Figure 5: Schematic representation of the ELS detector. ....	11
Figure 6: Degradation of GC.....	16
Figure 7: Graph showing which molar ratio of PNS has to be used to achieve targeted degree of palmitoylation.....	17
Figure 8: Palmitoylation reaction. ....	18
Figure 9: Graph showing the reaction times needed to achieve targeted degree of quaternization. ....	19
Figure 10: Quaternization of pGC.....	20
Figure 11: Avestin C5 homogenizer (38).....	24
Figure 12: Steri-Dropper™ Polyethylene Sterile Eye-Dropper Bottles.....	25
Figure 13: The results of GCPQ NMR analysis: A – CH <sub>3</sub> end of palmitic acid chain, B – palmitic acid chain, C – the second CH <sub>2</sub> in palmitic acid chain, D – acetyl peak, E – the first CH <sub>2</sub> in palmitic acid chain, F – tertiary and secondary amine, G – quaternary amine and H – the sugar backbone.....	30
Figure 14: Linearity of the CsA calibration curve.....	31
Figure 15: An example of HPLC chromatogram showing a well-defined CsA peak (c = 1,25 mg/mL). ....	31
Figure 16: Graph showing the increase of solubilised CsA through time. Samples were incubated at 4 °C and were constantly stirred with magnetic stirrer. ....	34
Figure 17: C2 sample - from left to right: 0, 1, 3, 5 and 21 hours of magnetic stirring at 4 °C.....	34
Figure 18: Graph representing distribution of particle sizes in sample A. Red curve represents the non-homogenized formulation. With increasing number of cycles (B0 – B35), a second population of larger particles appears.....	35
Figure 19: Graphical presentation of z-average values defined in samples of formulation after different numbers of cycles.....	36

Figure 20: Graph showing us how the peaks change with increasing numbers of homogenization cycles. Blue line represents the population of peak 1 (primary vertical axis) which does not change significantly after 5 - 10 cycles. However after 20 cycles the peak 2 population (secondary axis) appears, which then persists up to the 35<sup>th</sup> cycle... 37

Figure 21: Graphical presentation of DLS signal intensity coming from peak 1 population. The intensity fell under 90% after 15 cycles, when the 2<sup>nd</sup> peak population begins to appear..... 38

Figure 22: Graph showing the increase of PDI (Polydispersity Index) values with increasing number of cycles, which is a consequence of presence of the second peak population..... 38

Figure 23: The calibration curve of the GCPQ polymer. .... 39

Figure 24: Concentrations of GCPQ polymer in our formulations, after 30 days of their manufacturing, during which time they were kept at different conditions..... 39

Figure 25: Chromatogram showing the position of the CsA reference peak. .... 40

Figure 26: Chromatogram showing the position of the glycerol reference peak. .... 41

Figure 27: Chromatogram showing the position of the GCPQ peak. The inverted peak in the beginning of the chromatogram is a result of subtracting the blank run (control sample without GCPQ, containing only CsA). .... 41

Figure 28: Representative chromatogram of a formulation sample showing the position of the GCPQ peak. .... 42

Figure 29: Concentrations of CsA in 0,01% formulations during the course of the stability study carried out under different conditions..... 42

Figure 30: Concentrations of CsA in 0,02% formulations during the course of the stability study carried out under different conditions..... 43

Figure 31: Concentrations of CsA in 0,05% formulations during the course of the stability study carried out under different conditions..... 43

Figure 32: Graph representing the changes of osmolarity in formulations containing 0,01% CsA, during the course of stability study, carried out under different conditions..... 44

Figure 33: Graph representing the changes of osmolarity in formulations containing 0,02% CsA, during the course of stability study, carried out under different conditions..... 44

Figure 34: Graph representing the changes of osmolarity in formulations containing 0,05% CsA, during the course of stability study, carried out under different conditions..... 45

Figure 35: Graph showing changes in viscosity of formulations containing 0,01% CsA during the course of the stability study, carried out under different conditions.....	45
Figure 36: Graph showing changes in viscosity of formulations containing 0,02% CsA during the course of the stability study, carried out under different conditions.....	46
Figure 37: Graph showing changes in viscosity of formulations containing 0,05% CsA during the course of the stability study, carried out under different conditions.....	46
Figure 38: Graph showing changes in zeta potential of formulations containing 0,01% CsA during the course of the stability study, carried out under different conditions.....	47
Figure 39: Graph showing changes in zeta potential of formulations containing 0,02% CsA during the course of the stability study, carried out under different conditions.....	47
Figure 40: Graph showing changes in zeta potential of formulations containing 0,05% CsA during the course of the stability study, carried out under different conditions.....	48
Figure 41: Graph showing particle size distribution in a sample containing 0,01% CsA after 14 days of incubation at 5-6°C.....	49
Figure 42: Graphical presentation of peak 1 particle size changes (intensities) in formulations containing 0,01% CsA during the stability study, carried out at different conditions. ....	49
Figure 43: Graphical presentation of peak 1 particle size changes (intensities) in formulations containing 0,02% CsA during the stability study, carried out at different conditions. ....	50
Figure 44: Graphical presentation of peak 1 particle size changes (intensities) in formulations containing 0,05% CsA during the stability study, carried out at different conditions. ....	50
Figure 45: Stacked bar graphs showing the percentages of intensities of two peaks present within the particle population in formulations containing 0.01% CsA that were kept in fridge at 5 – 6 °C, for 28 days. ....	51
Figure 46: Stacked bar graphs showing the percentages of intensities of two peaks present within the particle population in formulations containing 0.01% CsA that were kept in fridge at room temperature (18 – 23 °C), for 28 days. ....	51
Figure 47: Stacked bar graphs showing the percentages of intensities of two peaks present within the particle population in formulations containing 0.01% CsA that were kept in incubator at 40 °C, for 28 days. ....	52

Figure 48: Stacked bar graphs showing the percentages of intensities of two peaks present within the particle population in formulations containing 0.02% CsA that were kept in fridge at 5 – 6 °C, for 28 days. ....	52
Figure 49: Stacked bar graphs showing the percentages of intensities of two peaks present within the particle population in formulations containing 0.02% CsA that were kept in fridge at room temperature (18 – 23 °C), for 28 days. ....	52
Figure 50: Stacked bar graphs showing the percentages of intensities of two peaks present within the particle population in formulations containing 0.02% CsA that were kept in incubator at 40 °C, for 28 days. ....	53
Figure 51: Stacked bar graphs showing the percentages of intensities of two peaks present within the particle population in formulations containing 0.05% CsA that were kept in fridge at 5 – 6 °C, for 28 days. ....	53
Figure 52: Stacked bar graphs showing the percentages of intensities of two peaks present within the particle population in formulations containing 0.05% CsA that were kept in fridge at room temperature (18 – 23 °C), for 28 days. ....	54
Figure 53: Stacked bar graphs showing the percentages of intensities of two peaks present within the particle population in formulations containing 0.02% CsA that were kept in incubator at 40 °C, for 28 days. ....	54
Figure 54: Graphical presentation of poly-dispersity index changes (PDI) in formulations containing 0.01% CsA during the course of the 28 days long stability study, carried out at different conditions. ....	55
Figure 55: Graphical presentation of poly-dispersity index changes (PDI) in formulations containing 0.02% CsA during the course of the 28 days long stability study, carried out at different conditions. ....	55
Figure 56: Graphical presentation of poly-dispersity index changes (PDI) in formulations containing 0.05% CsA during the course of the 28 days long stability study, carried out at different conditions. ....	56
Figure 57: Photography showing Petri dishes with TSB agar inoculated with bacteria, samples of our formulations and negative controls. For detailed explanation, please see Table VIII. ....	60

## ABSTRACT

Eye drops are most common formulation used to treat ophthalmic diseases. Despite novel formulations coming to market, liquid solutions and suspensions of ophthalmic drugs represent the most patient-compliant way to deliver them to the eye. As the eye can get easily irritated, it is important, that eye drops have characteristics that mimic tears, which are mostly composed of water. However, some molecules, for example cyclosporine A, that we used in our formulation, do not solubilize in water, therefore we need to use hydrophobic solvent to improve its solubility.

Nanoparticles can also be used for delivery of hydrophobic drugs. Quaternary ammonium palmitoyl glycol chitosan (GCPQ) nanoparticles are self-assembled polymeric micelles that can be loaded with hydrophobic, as well as hydrophilic drugs and have shown good results not only in ophthalmic, but also in oral and intravenous delivery routes.

Nowadays, there are many particle homogenization methods available, however not all of them can be used on the industrial scale. For example, high pressure homogenization can be used for high scale production, and the whole process can be thermally controlled.

To be able to bring a new formulation on the market, it needs to undergo a number of tests to prove its safety, efficiency and stability. One month stability test under different conditions is one of the first steps within this process. We used this important test following a successful synthesis of the GCPQ polymer and optimization of the cyclosporine A containing nanoparticle production process to evaluate stability characteristics of this new eye drop formulation. By using high pressure liquid chromatography (HPLC), we have shown that the quantity of the GCPQ polymer remained unchanged through the stability test. Additionally we were able to partly carry out the sterility test according to the United States Pharmacopeia (USP), due to the fact that we did not have all required bacterial lines available.

.

**Key words:** eye drops; nanoparticles; cyclosporine A; quaternary ammonium palmitoyl glycol chitosan (GCPQ); stability

## POVZETEK

Kapljice za oči so še vedno najbolj uporabljan dostavni sistem za zdravljenje bolezni oči. Kljub novjšim farmacevtskim oblikam, ki prihajajo na trg, so kapljice za oči še naprej dobro sprejete s strani pacientov. Oko je občutljiv organ, ki se lahko hitro razdraži, zato je zaželeno, da imajo kapljice podobne lastnosti kot solze, v katerih prevladuje voda. Nekatere zdravilne učinkovine, ki se uporabljajo v oftalmologiji pa niso topne v vodi, zato moramo za njihovo raztapljanje in dostavo na oko uporabiti ustrezen hidrofoben vehikel. Med hidrofobne zdravilne učinkovine sodi tudi imunosupresiv ciklosporin A, ki smo ga uporabljali v naših poskusih.

Nanodelci so eden od novjših dostavnih sistemov v vodi slabo topnih učinkovin. Nanodelci kvarternega amonijevega palmitoil glikol hitosana (GCPQ) nastanejo v vodi spontano na podlagi tvorbe polimernih micelov. Vanje lahko vgradimo tako hidrofobne kot hidrofilne učinkovine, pokazali pa so dobre rezultate tako pri dostavi učinkovin v oko kot tudi pri peroralni in intravenski aplikaciji različnih učinkovin. Zato smo nanodelce GCPQ izbrali kot nosilni sistem za izdelavo kapljic za oči s ciklosporinom A.

Uniformnost delcev v koloidni disperziji dosežemo s homogenizacijo. Ena od možnih metod je visokotlačna homogenizacija, ki se lahko, poleg rotor-stator homogenizatorjev uporablja tudi na industrijskem nivoju. Poleg tega pa visokotlačno homogeniziranje omogoča tudi izvedbo nadzora temperature skozi celoten proces. Zaradi omenjenih lastnosti, smo to metodo uporabili za pripravo naše formulacije.

Razvoj nove formulacije zahteva veliko eksperimentalnega dela in izvedbo številnih testov kot delov študij, s katerimi dokazujemo njeno varnost, učinkovitost in stabilnost. Enomesečna stabilnost kapljic za oči je eden od prvih korakov ugotavljanja stabilnosti formulacije, zato smo z njo v treh paralelkah testirali našo formulacijo s ciklosporinom A, pri čemer smo uporabili tri različne temperature in tri različne koncentracije učinkovine. Pred izdelavo končne formulacije pa smo optimizirali celoten tehnološki proces izdelave in mu dodali korak za večji izkoristek vgradnje učinkovine. Pri kapljicah za oči je zelo pomembno, da je končni izdelek sterilen. To smo dosegli s filtracijo formulacije skozi 0.22 µm filter v sterilne plastične kapalke v sterilnem okolju. Test sterilnosti smo izvedli skladno z zahtevami ameriški farmakopeje, pri čemer pa smo ga, zaradi nerazpoložljivosti nekaterih predpisanih bakterijskih linij z vidika dokazovanja primernosti kombinacije

medija in pripravka za rast aerobnih in anaerobnih mikroorganizmov, lahko opravili le delno.

Optimizacija celotnega procesa nam je dobro uspela, saj smo iz prvotnih 30 ciklov homogenizacije prišli na le 10 – 15 ponovitev ter tako prihranili čas in energijo. Rezultati testa enomesečne stabilnosti so pokazali, da je bila naša formulacija stabilna pri nizki temperaturi. Za vse vzorce, testirane pri višjih temperaturah pa tega ne moremo potrditi ali ovreči, saj so spremembe značilnosti formulacije lahko posledica napak, ki smo jih storili med analiznim postopkom. Za stabilno formulacijo je zelo pomembno, da ohrani količino polimera, v katerega je vgrajena učinkovina. Z metodo HPLC smo dokazali, da se količina polimera GCPQ tekom testa enomesečne stabilnosti ni spremenila.

**Ključne besede:** kapljice za oči; nanodelci; ciklosporin A; kvarterni amonijev palmitoil glikol hitosan (GCPQ); stabilnost

## LIST OF ABBREVIATIONS

<b>Abbreviation</b>	<b>Meaning</b>
BBB	Blood-brain barrier
CD <sub>3</sub> OD	Deuterated methanol
CsA	Cyclosporine A
Da	Dalton
dGC	Degraded glycol chitosan
DLS	Dynamic light scattering
DMSO	Dimethylsulfoxid
DP	Degree of palmitoylation
DQ	Degree od quaternization
ELSD	Evaporative light scattering detector
GC	Glycol chitosan
GCP MALLS	Gel permeation chromatography Multi Angle Laser Light Scattering
GCPQ	Quaternary Ammonium Palmitoyl Glycol Chitosan
HCl	Hydrochloric acid
HPH	High pressure homogenization
HPLC	High pressure liquid chromatography
IL	Interleukin
IOP	Intra ocular pressure
kDa	Kilo Dalton
LC	Liquid chromatography
MeI	Methyl iodide
MW	Molecular weight
NaOH	Natruim hydroxide
NEt <sub>3</sub>	triethylamine
NMP	N-methylpyrrolidone
NMR	Nuclear magnetic resonance
PGC	N-palmitoyl glycol chitosan
PNS	Palmitic acid N-hydroxysuccinimide ester

ppm	Particles per million
psi	Pounds per square inch
SD	Standard deviation
TSB	Tryptone Soya Broth
UK	United Kingdom
USA	United States of America
USP	United States Pharmacopeia
WHO	World health organization
ZP	Zeta potential

## 1. INTRODUCTION

Eyes are important organs for a high quality of life. Together with cancer, Alzheimer disease and HIV/AIDS, blindness ranked in top four “worst things that could happen to you”, based on a survey made among Americans. Today, many causes which can lead to vision impairment or blindness can be successfully treated either with medicines or surgery. Based on the World Health Organization (WHO) 2014 data, 80% of visual impairments can be either cured or prevented. However, this is not an excuse for not taking care of our eyes. Actually, it must be our priority to educate people, how important it is to take care of their health and to follow the treatment instructions, because it can happen that what was taken for granted (health), can quickly turn into a privilege (1, 2).

### 1.1.Eyes

Eyes are quite sensitive parts of human body. However, they possess many defence mechanisms, which prevent them from getting infected or injured. Eyelids are the very first line of eye protection which do not only reduce excessive light entering the eyes and defend them from particles in the air, but also moisture and spread tear film equally over their whole surface. Additionally, every eyelid has at its very end eyelashes, which more or less successfully protect eye surface from dust and other debris that might cause eye irritation. Actually, eyelashes are sensitive sensors, as touching one of their hairs stimulates receptors that trigger the blink reflex and the eye is closed instantly (3, 4).

The conjunctiva covers almost the whole anterior surface of the eye, while the very front part of the eye is covered with cornea. Conjunctiva also covers the inner surface of the eyelid. Its function is to secrete mucous film that prevents the eyeball from drying. Sclera and cornea are both parts of a fibrous layer. Sclera, also known as “white of the eye”, which is made of collagen and contains nerves and blood vessels, covers almost the whole eye surface. The sclera’s structure changes in the front part of the eye, where it forms cornea that covers the anterior eye chamber and allows light to enter the eye. As cornea is transparent, the light can pass through the lens onto the fotoreceptors of retina which then enables vision (3, 4).

The tear film together with the lacrimal apparatus is more a protective system than a component of the eye. Tears are produced within the lacrimal gland. They bring nutrients

and oxygen to the conjunctiva, wash away foreign particles and waste that have no place to be in the eye and lubricate the surface. Furthermore, they reduce torsion during blinking and eye movements and protect eyes against environmental challenges, such as wind and cold. Tears are essential for maintaining transparency and health of cornea. An important ingredient of tears is *lysozyme*, the enzyme whose bactericidal function is vital in preventing and fighting infections which might endanger the health of the eye. Eyelid blinking pushes tears across whole surface to the lacrimal punctum located at the other side of the eye. From there they enter a canal leading to the lacrimal sac, from where they travel via nasolacrimal duct to nasal cavity (3, 4).

Unfortunately, as everything else in our bodies, the eyes' defence systems and mechanisms are also not absolute, as they can get damaged by infections or other causes, which significantly reduce their important defence functions (3, 4).

## 1.2. Eye diseases and epidemiology

There are many diseases threatening this important and sensitive organ. We can divide them in two groups, i.e. those affecting the inner eye and those affecting the external eye. We will focus on those affecting the eye surface, where many of them can be efficiently cured with medicines. Diseases of the external eye affect the visible parts of the eye, conjunctiva, cornea, sclera, eyelid and two liquid flow systems, the lacrimal and aqueous humour flow (5).

A disease that affects 6 million people in the USA annually is conjunctivitis. Viral eye infections are the most common cause (80%) of all acute conjunctivitis. Still, 50% of viral conjunctivitis cases are misdiagnosed as being caused by bacteria. Bacterial infections are the main cause for acute conjunctivitis in children and its annual incidence is 135 per 10.000 in a whole population. Bacterial or viral infections cause inflammation of the conjunctiva and include symptoms like bursting sensation in eyes, sticky coating on the eyelashes and enlarged lymph nodes in front of the ear. When infection is more severe antibiotic eye drops need to be applied. On the other hand, non-infectious conjunctivitis can either be a result of allergic reaction or it can be associated with some external chemicals or toxins. It presents itself as eye redness and itchiness. Allergic conjunctivitis is treated with antihistamines (5, 6, 7).

Corneal ulcers are caused by wearing contact lenses or by different infections. Based on a study carried out in Northern California, 27,6 out of 100.000 people develop this disease annually. However this number is significantly higher, when patients are wearing contact lenses and it reaches 130, 4 per 100.000 people. Immediate and effective treatment is really important otherwise corneal ulcers can lead to more serious complications, such as severe vision loss or corneal scars. When the treatment is unsuccessful, it is still possible to transplant donated corneal tissue (5, 8, 9).

Eye dryness in the first place brings up a really annoying feeling of having sand or other foreign particles in our eyes. In this case it is important to replace lack of tear film with artificial tears or tear ointments. If this is not done, eye dryness can cause severe damage of cornea and conjunctiva. Depending on the severity of disease more or less aggressive treatments may be used. Epidemiological data gathered before 2008 show that the prevalence of dry eye disease can really differ depending on the geographical region and risk factors, such as smoking, sex, weather conditions and age. The prevalence of disease is estimated to be 7,4% - 33,7%, depending on the study, the way the disease was diagnosed and which population was surveyed (5, 10).

An important cause of vision impairment and blindness is glaucoma. Glaucoma means that ocular tissue is at least partly damaged by high intra ocular pressure (IOP). Higher than normal IOP is caused by obstructed aqueous humour flow from ciliary body to trabecular meshwork. In the so-called angle-close glaucoma the iris closes this path, due to its moving towards trabecular meshwork. This form of disease had a prevalence of 1,6 million people in Europe and 130.000 in the UK in year 2012. The flow of aqueous humour can also be misdirected, as instead of flowing to the aqueous chamber it might flow into the vitreous cavity, pushing the iris, lens and the vitreous tissue forward. Aside to closed angle glaucoma, the open angle glaucoma also exists. In this case the optical nerve is damaged due to elevated IOP, however no abnormalities are found on ophthalmic examination. Medical treatment is aimed at preserving the vision, so first, the IOP must be lowered. It is also important to enhance patient's overall health and provide the best possible treatment. Glaucoma can be treated with various medicines, usually applied in the form of eye drops, or with incisional or laser surgery, when pharmacotherapy is insufficient. There are many substances that can lower IOP:  $\beta$ -blockers,  $\alpha$ -agonists, miotic agents, prostaglandin analogs

and carbonic anhydrase inhibitors. Glaucoma causes full vision loss in 8% of cases worldwide (11, 12).

Episcleritis is an inflammatory condition of the episclera. As it is self-limiting, usually no special treatment is needed. However in case of severe disease, topical steroids and oral anti-inflammatory agents may be used. On the other hand, the anterior scleritis involves inflammation of sclera, overlying conjunctiva and episclera, therefore systemic treatment with anti-inflammatory agents is necessary. In severe cases oral steroids are prescribed, because their topical use is ineffective. For both pathological conditions a study of their incidence and prevalence has been made in Northern California. The annual prevalence rate of episcleritis was found to be 52,6 per 100.000 people and that of scleritis, 5,6 per 100.000. Furthermore, the overall incidence of episcleritis was 41,0 and that of scleritis 3,4 per 100.000 people (5, 11, 13).

### 1.3. Formulations for treatment of eye diseases

Ophthalmic delivery systems are quite a challenge for pharmaceutical technology. The biggest obstacles we face are the eye's defence mechanisms. Cornea has naturally hydrophobic surface, therefore this obstacle has to be overcome by tears in order to completely cover the cornea. As mucin, present in tears changes its hydrophobic surface into a hydrophilic, it is actually much easier to deliver hydrophilic than hydrophobic drugs through the eye surface. To successfully overcome all ocular barriers, many different formulations and drug delivery systems have been developed for treating different ophthalmic diseases. In a conventional ocular delivery systems group we have solutions/liquids, emulsions, suspensions and ointments. The most convenient ones among them are liquids and solutions, as they are safe, immediately active, patient compliant and non-invasive. Various additives, such as viscosity and permeability enhancers and cyclodextrins, are often added to them in order to improve contact time, permeation and ocular bioavailability. All other conventional formulations for ophthalmic use were developed to improve solubility, pre-corneal residence time and ocular bioavailability of drugs. On the other hand, various side effects are associated with these formulations, such as irritation, redness, inflammation, blurred vision, inflammation and there are also stability issues (14, 15, 16).

Novel drug delivery systems are in many cases based on nanotechnology. Namely, some of nanocarriers have shown good results in enhancing ocular bioavailability. These are nanomicelles, nanoparticles, nanosuspensions, liposomes and dendrimers. Nanoparticles have raised quite an interest in ocular delivery and researchers have attempted to deliver drugs loaded nanoparticles to anterior, as well as posterior ocular tissues (14, 15, 16).

Other novel formulations are in-situ gelling systems, where the gelation of formulation can be triggered by a temperature or pH change, or even by UV radiation. Special eye inserts or implants that keep drugs in the eye for a longer time are also being introduced but they must be inserted and removed by a doctor, unless they are biodegradable. To prolong the presence of drugs on eye surface, special drug containing contact lenses are also used. The use of micro-needles is a novel technique for treatment of posterior eye diseases. It is minimally invasive and reduces the risk of many complications, such as retinal detachment, haemorrhage, cataract, etc. (14, 15, 16).

#### 1.4. Formation of nanoparticles (homogenization)

High pressure homogenization (HPH) is a method used for preparing nano-scale particles and providing their monodispersity. The process is completely mechanical. In HPH the fluid to be homogenized gets under the impact of high pressure while being pushed through a narrow gap, where it starts to flow with supersonic speed (Figure 1). It undergoes the *impact* when the tube starts to become narrower. *Sheer forces* are in operation while the fluid flows through the narrow part of the tube, and when it leaves the narrow tube, *cavitation* occurs. Through this process droplets are reduced from micro- to the nano-scale range. Parameters that affect the efficiency of HPH are: pressure, temperature, number of fluid passes, valve and impingement design, as well as and flow rate. (17,18).

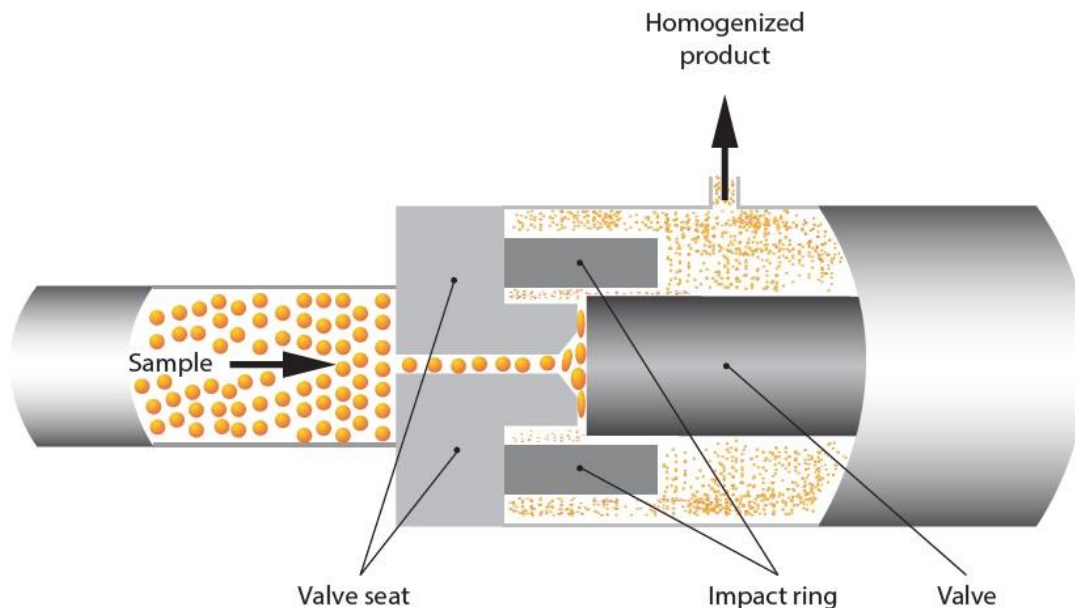


Figure 1: Schematic presentation of an HPH cell.

### 1.5. Quaternary Ammonium Palmitoyl Glycol Chitosan (GCPQ)

N-palmitoyl-N-monomethyl-N,N-dimethyl-N,N,N-trimethyl-6-O-glycolchitosan (GCPQ) is a polymer, derived from a glycol chitosan (GC) (Figure 2). It is synthesised by a carbohydrate backbone modification with hydrophilic and hydrophobic groups, thereby creating an amphiphilic polymer. At low micellar concentrations in aqueous media, the polymer self-assembles and creates 100 – 300 nm clusters of smaller, 10 – 30 nm large micellar aggregates. Due to its properties, the GCPQ polymer belongs to a group of polysoaps which are well known solubilizing agents (19, 20, 21).

The GCPQ polymer is not only an efficient solubilizing agent, but it also significantly enhances absorption of orally administered hydrophobic drugs. The the absorption of orally taken drugs is limited by their high molecular weight (>500 Da), high log P values (>2.0) and low gastrointestinal permeability. A representative of such substances is cyclosporine A, whose  $C_{max}$  value increases 5-times when administered with the GCPQ polymer. The main reason for increasing the absorption of drugs with GCP is their increased dissolution, adherence to and penetration through the mucous layer and enhancement of the transcellular transport. Furthermore, with the development of peptides

for therapeutic use, a great challenge to transport them through the gastrointestinal mucosa and blood-brain barrier (BBB) arose. When stabilized with GCPQ polymer, they are protected from gastrointestinal degradation and can be transported across enterocytes to the systemic circulation, from where they are able to enter the brain (22, 23).

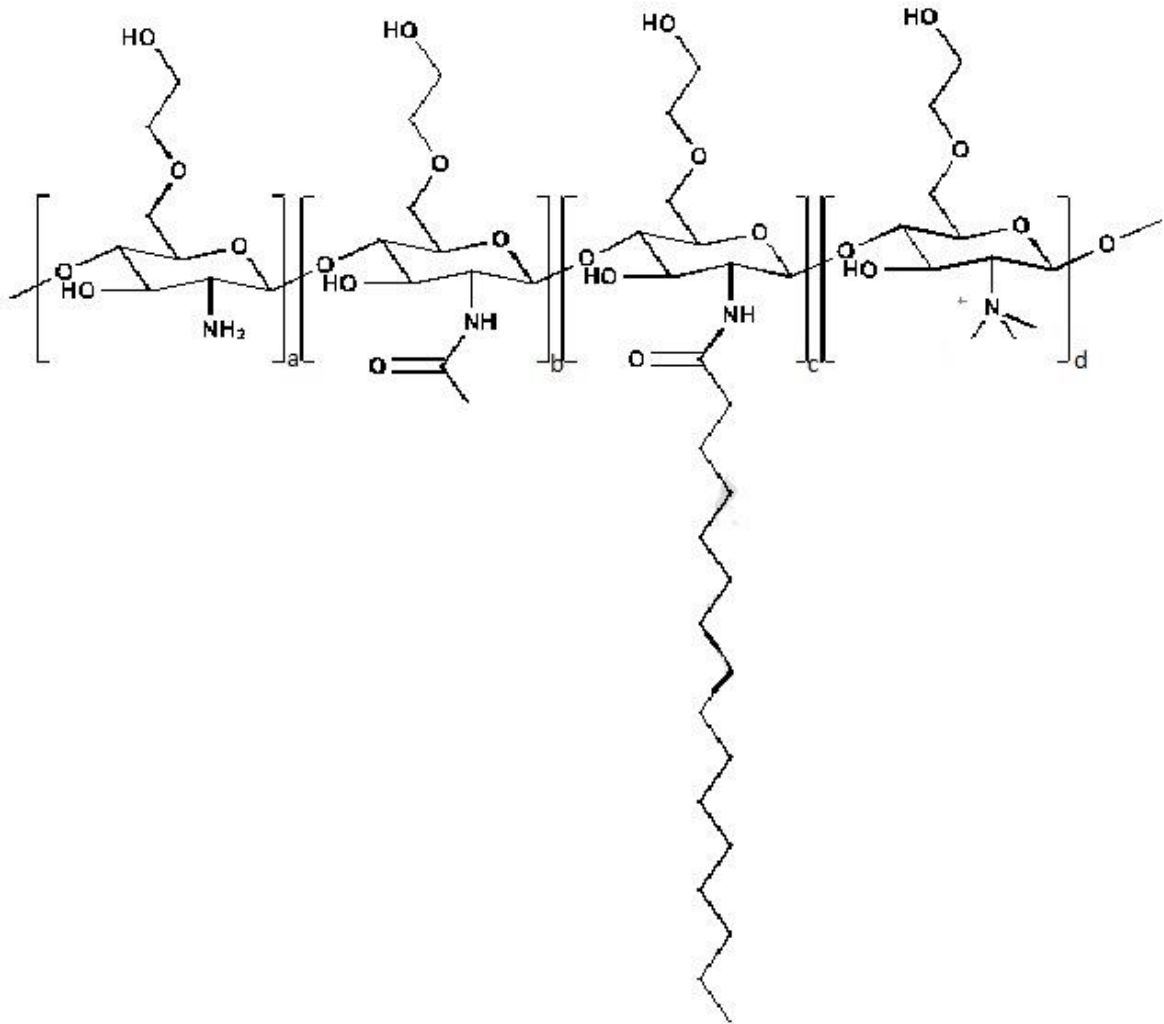


Figure 2: The chemical structure of GCPQ.

### 1.6. Cyclosporine A (CsA)

Cyclosporine A is a natural lipophilic cyclic undecapeptide isolated from the fungus *Hypocladium inflatum gams* (Figure 3). Due to its immunosuppressive activity, it has been widely used for treatment of allograft rejection and graft vs. host disease following allogeneic organ and hematopoietic stem cell transplantation. Cyclosporine A inhibits transcription of cytokine (including IL-2 and IL-4) genes in activated T cells. T cells are part of adapted immune system and play a central role in recognizing and eliminating

foreign matter. As transplanted allogeneic organs and tissues are foreign to our recipients, CsA is used as immunosuppressive agent to prevent graft rejection. However, CsA has many side effects, as it also exerts neuro-, nephro- and hepatotoxicity (24).

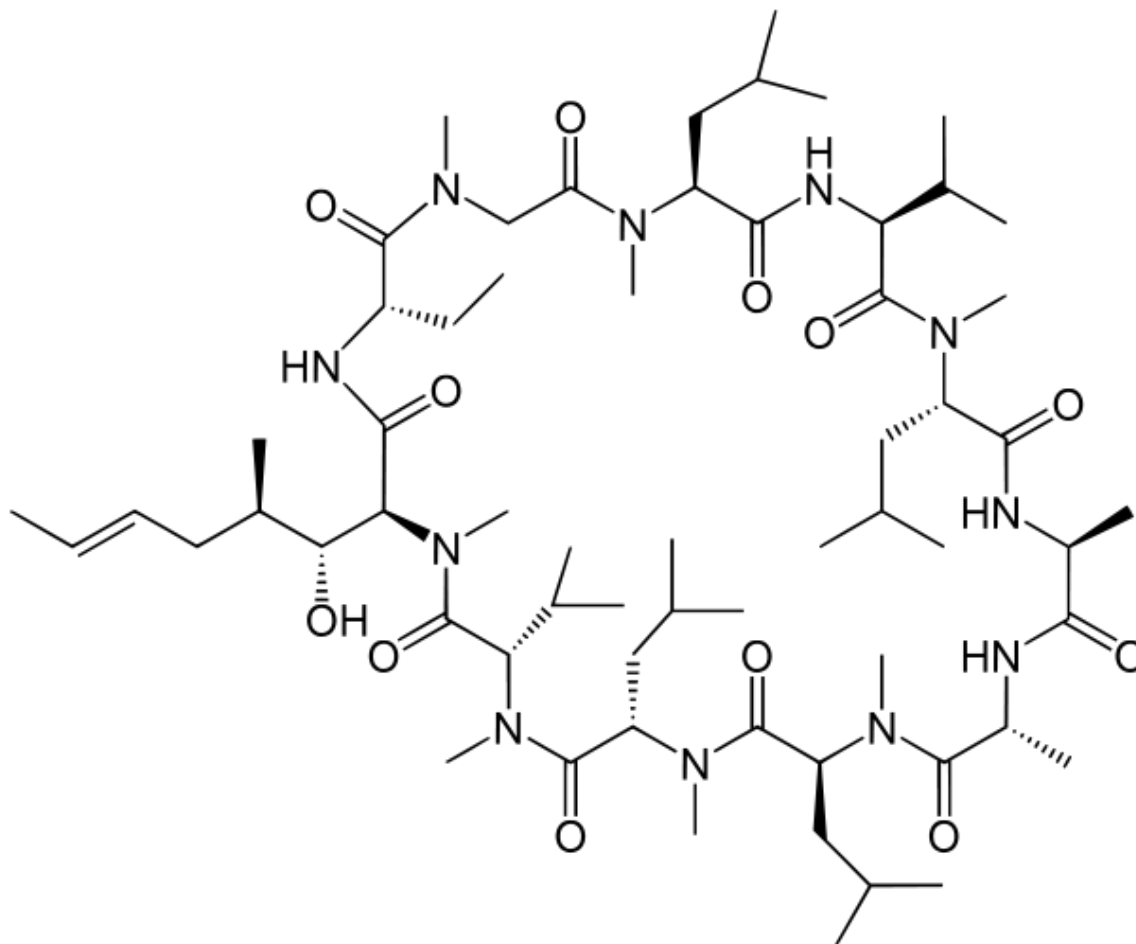


Figure 3: Chemical structure of Cyclosporine A (25).

## 1.7.Characterization of formulations

### 1.7.1. Dynamic Light Scattering (DLS)

Dynamic Light Scattering (DLS), also known as Photon Correlation Spectroscopy is widely used to measure sizes of small particles, usually smaller than 1.000 Da. This scattering technique is based on Brownian motion (pedesis) of particles and measures their diffusion. When light hits a particle it is scattered in all directions and the intensity of scattered light is determined by the size of a particle. When conditions of random walk and

spherical shape of particles are accomplished, we can calculate their average diameter using the Stokes-Einstein relation. As bigger particles scatter light more than the smaller ones, the sensitivity of DLS to impurities represents a major problem, giving erroneous results.

The main advantages of this technique are: small volume of sample needed, fast measurements and ease of use. On the other hand, we must be careful when analysing results. By applying the Mie theory we can convert data from intensity size distribution (based on particle light scattering) to volume and number size distribution where distribution (based on particle volume and mass). However, such results can only be used for comparative analysis and should not be considered as absolute values (26, 27, 28).

### 1.7.2. Zeta potential

When looking at the stability of particles in suspension one of the main parameters to be considered is zeta potential (ZP). Particles in a suspension can possess surface charge. The surface layer of particles can be divided in two parts. The first one is the inner region, also called Stern layer, where ions are strongly bound to particle surface. The second one is the outer region or diffusion layer, where ions are bound to the particle surface more loosely. When the particle moves, the ions on the stable side of diffusion layer move with it. The charge on the boundary, where stable ion formation on the particle surface ends, is called zeta potential (29, 30, 31).

For suspension to be stable it is important that its ZP is either highly positive or negative. In this case particles will not be attracted to themselves and they will not aggregate. On the other hand, if the ZP value is low there is no force that would prevent particles from colliding and forming aggregates. A suspension is considered stable when its ZP is higher than +30 mV or lower than -30 mV (29, 30, 31).

### 1.7.3. Osmolarity

Osmolarity or osmotic concentration is determined by the amount of substance that has osmotic activity in a solution. Actually it is the concentration of solutes in osmoles per litre of solution (32).

In our experiments we used the freezing point depression technique to measure the osmolarity of our eye drops formulations (Figure 4). With this technique we compare the osmolarity of a given sample to pure water. The sample in a plastic tube is cooled on one side and warmed on the other. The sample temperature is measured during osmolarity determination. After super cooling of sample, a needle is placed into it to initiate freezing and sample become partly crystallized. Heat of fusion raises samples temperature and the freezing point is reached. Placing a needle into a sample is important for reproducibility of measurements (33).

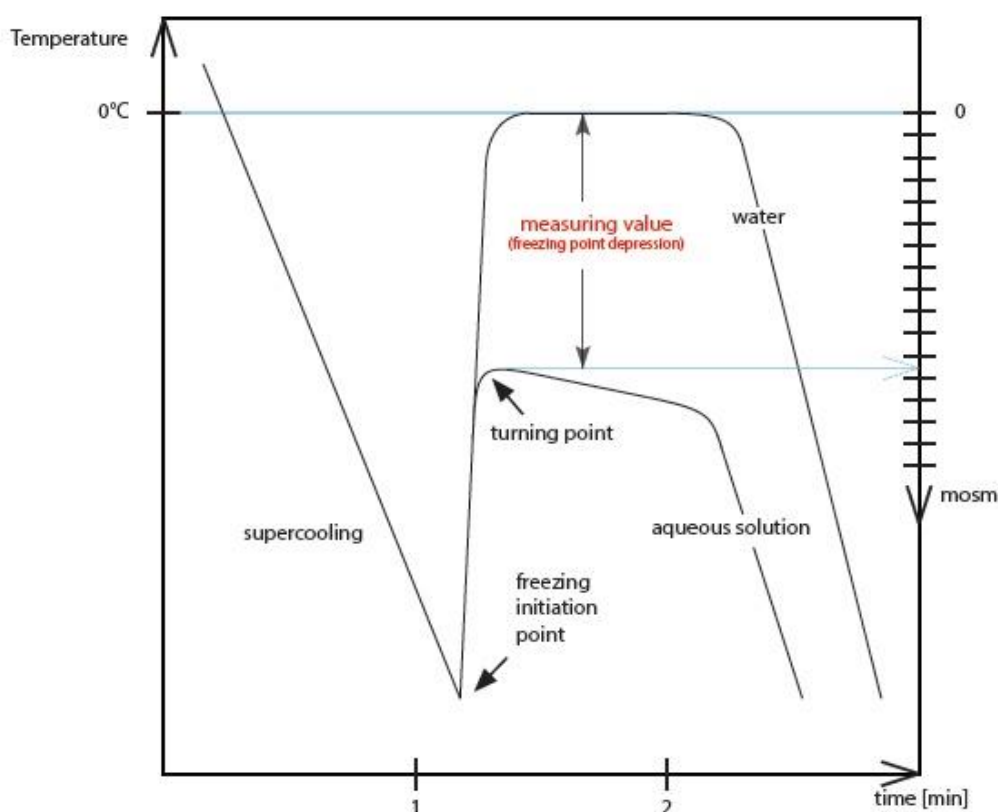


Figure 4: Graph, representing the principles of freezing point depression technique.

#### 1.7.4. Viscosity

Viscosity is a physical property of a fluid. It is caused by shear stress when surfaces of two fluids are moving at different velocities. Also, when a fluid is forced through a tube, stress

causes friction between its different layers. Pressure builds up because molecules near tube walls are moving slower than those near tube axis (34).

Same friction is also present under eyelids while blinking. This is the reason why it is good to know viscosity of an eye formulation. Still we could argue what viscosity would be the best for eye drops. On one hand, if it is too low, the formulation is easily washed away, on the other hand if it is too viscous it blurs vision for a longer time and is irritating.

#### 1.7.5. Evaporative light scattering detection (ELSD)

Evaporative light scattering detector (ELSD) (Figure 5) is used in high pressure liquid chromatography when non- or semi-volatile substances are analysed. Furthermore, ELSD is also used when analytes have no UV chromophores. The detection process is divided into three stages. First, the eluent is nebulized, which means that the liquid becomes an aerosol at defined temperatures. For this to be achieved inert gas is used which forms uniform droplets of liquid. Then the aerosol passes through a temperature-controlled evaporator tube, where the solvent is removed. Less volatile particles are left behind and pass through the detection chamber. A light source falls on particles and the scattered light detected is proportional to the mass of a solute (35, 36).

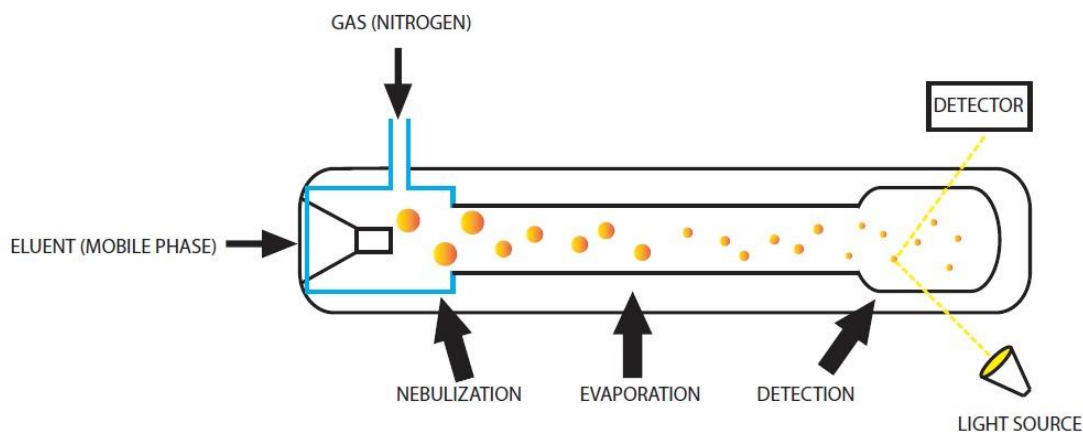


Figure 5: Schematic representation of the ELS detector.

## 2. AIMS AND OBJECTIVES

- To synthesize and characterize GCPQ polymer that will be used for production of eye drop formulations.
- To prepare eye drops with three different concentrations (0.01%, 0.02% and 0.05%) of cyclosporine A (CsA), using the homogenization method.
- To perform stability tests of eye drops over 28 days period, at three different temperatures and 3 replicates for each CsA concentration, by measuring cyclosporine A concentration, viscosity, osmolarity, zeta potential and particle size.
- To optimize the procedure of eye drop formulation.

### 3. MATERIALS AND METHODS

#### 3.1. Materials:

Amberlite 410 (Sigma Aldrich, USA), Steri-Dropper™ Polyethylene Sterile Eye-Dropper Bottles (Helapet Limited, UK), Dialysis Tubing (3.5kDa) (Sigma Aldrich, USA), Microbiology Anaerocult® IS (Merck, Germany), Tryptone Soya Broth (Oxoid, UK), disposable cuvette DTS1070 and disposable 40µL cuvette (Malvern, UK)

#### 3.2. Solvents:

Acetone, Acetonitrile, Deionized water, Milli-pore double deionized water, Methanol, Diethyl ether, Deuternized water, Methanol-D4, Dimethyl sulfoxide, Isopropyl Alcohol.

#### 3.3. Reagents:

Glycol Chitosan, Sodium hydroxide, Palmitic acid *N*-hydroxysuccinimide ester, Hydrochloric acid, Glacial acetic acid, Methyl iodide, Anhydrous sodium acetate, Sodium iodide, Triethylamine, *N*-methylpyrrolidone, Cyclosporine A, Formic acid

Organisms: *Staphylococcus aureus* (NCTC 12923, UK), *Bacillus subtilis* (NCTC 8236,UK), *Pseudomonas aeruginosa* (ATCC 10662, UK) and *Escherichia coli* (NCTC 10419,UK ).

The solvents and reagents used were purchased from Fisher Scientific UK Ltd, Sigma Aldrich Chemical Co. (USA) and Wako (Japan), if not specified otherwise.

#### 3.4 Instruments:

- Agilent 1260 Infinity Series HPLC with Agilent 1290 Infinity II Evaporative Light Scattering Detector (ELSD), Agilent technologies, USA.
- Agilent 1200 Series HPLC with UV detection, Agilent technologies, USA.
- Avestin C5 Homogenizer , Avestin, Canada.
- Bruker Avance 400 MHz NMR spectrometer with broadband and selective (<sup>1</sup>H and <sup>13</sup>C) inverse probes, Bruker, USA.
- Zetasizer Nano series (Nano ZS), Malvern Instruments, UK.
- MICRO-Osmometer Type 5R, Roebing, Germany.

- M-VROC™ VISCOMETER, RheoSense, Inc., USA.
- GPC-Malls equipped with: Dawn Heleos II MALLS detector (120 mW solid-state laser operating at 658 nm), Optilab rEX interferometric refractometer (flow cell: 7.4  $\mu$ L at 658 nm), quasielastic light scattering (QELS) detectors (Wyatt Technology Corporation, Santa Barbara, CA, USA), and Agilent 1200 auto sampler (Agilent Technologies, UK).

### 3.5.Synthesis of GCPQ

#### 3.5.1. Degradation of glycol chitosan (GC)

To prepare degraded GC (dGC) we weighed out 25 g of high MW GC and added 4M HCl at room temperature to obtain the final concentration of 52 mg/mL (Figure 6). The starting amount of GC depends on quantity of GCPQ we want to prepare. The 4M HCl was prepared using 10M HCl, diluting it with deionized water. The solution of GC in 4M HCl was shaken for 8 hours (degradation time was predetermined, using data from Table I) at 100-125 rpm in a water bath at 50°C.

Table I: Guide to determine GC degradation.

<b>Reaction Time</b>	<b>Molecular Weight</b>
<b>(h)</b>	<b>(kDa)</b>
0-1	80 - 120
2	35 - 45
16-24	8,5 - 12
48	6,8 - 8,5
Redegradation of GC48 for 9h	2,8 - 4

When degradation process was completed, reaction was stopped by placing the flask under cold water for few minutes. The reaction mixture was then placed into a pre-soaked dialysis tubing (regenerated cellulose, molecular weight cut off 3.5 kDa) and dialyzed against 5L of deionized water over 24h, with at least 6 changes of dialysate (1-2 hours between each change). To detect the completion of dialysis we used a conductance meter, where values < 40  $\mu$ s should be reached. The dialysate was snap-frozen and placed in a freeze-drier for lyophilisation which took 48 h, resulting in a white coloured solid.

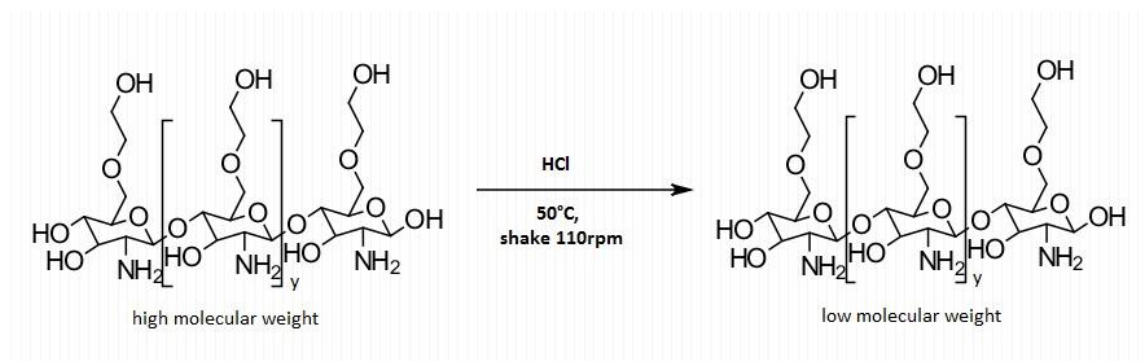


Figure 6: Degradation of GC.

### 3.5.1. Palmitoylation of degraded glycol chitosan (dGC) to N-palmitoyl glycol chitosan (pGC)

The product was further used for palmitoylation reaction. To 10g of the solid product 30 mL of DMSO per 1g of dGC was added and the mixture magnetically stirred at room temperature. Finally  $\text{NEt}_3$  (1.15mL per 1g of dGC) was added to the mixture. To obtain the targeted degree of palmitoylation (DP) we used data from Table II and Figure 7 to define exact molar equivalents of palmitic acid N-hydroxysuccinimide ester (PNS) to be added. The average MW for dGC (242,68 g/mol) and the average MW of PNS (353,5 g/mol) were used to calculate the appropriate molar ratio.

Table II: Guide to obtain the targeted degree of palmitoylation.

Molar equivalents of PNS	DP (%)	SD
0.05	4.2	0.1
0.10	8.2	0.1
0.15	12.5	0.8
0.20	16.0	0.2
0.22	18.0	-
0.25	20.2	1.2
0.50	33.6	1.5
0.75	42.9	4.2
1.00	50.6	5.4

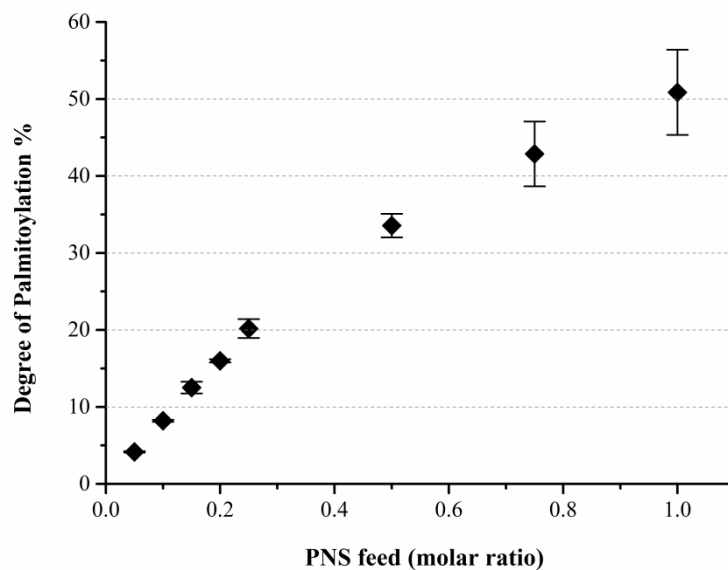


Figure 7: Graph showing which molar ratio of PNS has to be used to achieve targeted degree of palmitoylation.

The reaction mixture was stirred overnight, for at least 18h, at room temperature. Next day the reaction was completed (Figure 8) and the pGC was precipitated after adding 150 mL of the 1:2 mixture of acetone and diethyl ether per 1g of dGC. The product was left to settle down overnight after which it was washed 2 times with acetone (50 mL per 1g of dGC) and 2 times with diethyl ether (50 mL per 1g of dGC). Finally the product was filtered (filter porosity 3) and dried in vacuum for 24 hours at room temperature.

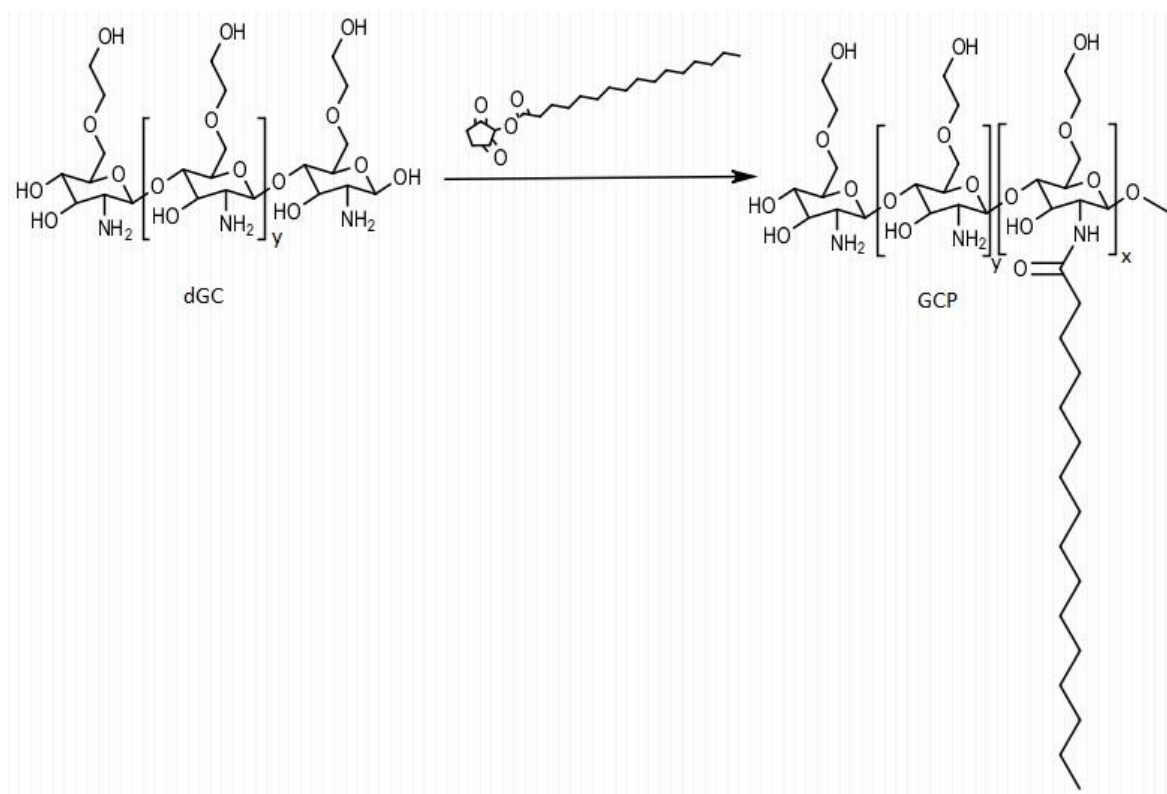


Figure 8: Palmitoylation reaction.

### 3.5.2. Quaternization of pGC

A proper quantity of the obtained pGC (10 g) was transferred into a flask and N-methylpyrrolidone (NMP, 80 mL per 1g of pGC) was added. The resulting mixture was stirred with magnetic stirrer for 3h. Subsequently powdered NaOH (0.13g per 1g of pGC) was poured into the reaction mixture which was stirred for another 40 min. After that, NaI (0.154 g per 1g of pGC) was added during stirring and at the same time the saturation of atmosphere in the flask with nitrogen gas was started. After 10 min MeI (1.5 mL per 1g of pGC) was added into the reaction mixture and the flask was placed on the pre-warmed water bed (36 °C). From this point we stirred the mixture for quite some time to achieve the desired degree of quaternization (Figure 9).

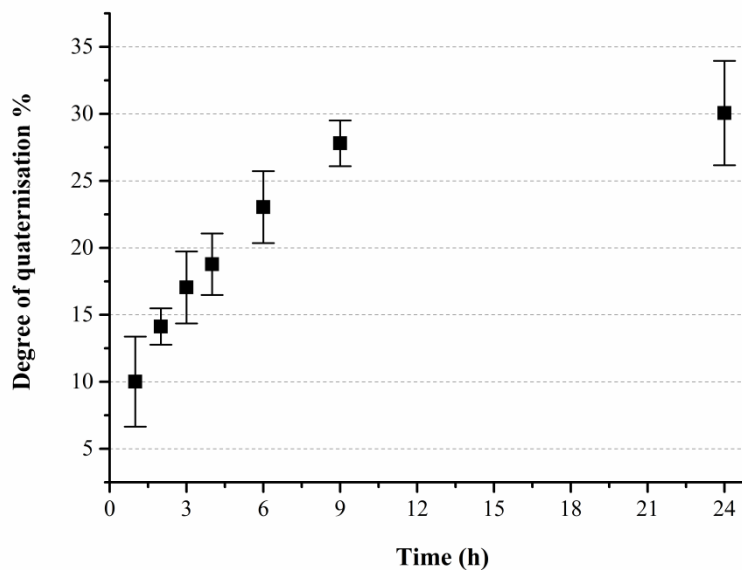


Figure 9: Graph showing the reaction times needed to achieve targeted degree of quaternization.

Finally the reaction (Figure 10) was stopped (after 3h) and the polymer was precipitated by adding the reaction mixture to diethyl ether (400 mL per 1g of pGC). It was left overnight to settle. The next day we observed gum formation which was actually our polymer. After decanting supernatant, the polymer was washed one more time with diethyl ether and then dissolved in methanol. The resulting solution was transferred into a dialysis tube with a 3.5 kDa cut-off and dialysed against 5 L of deionized water for 24 h. During dialysis the water was changed at least 6 times. In order to determine the end of the process, conductance meter was used, where values  $< 10 \mu\text{S}$  had to be observed.

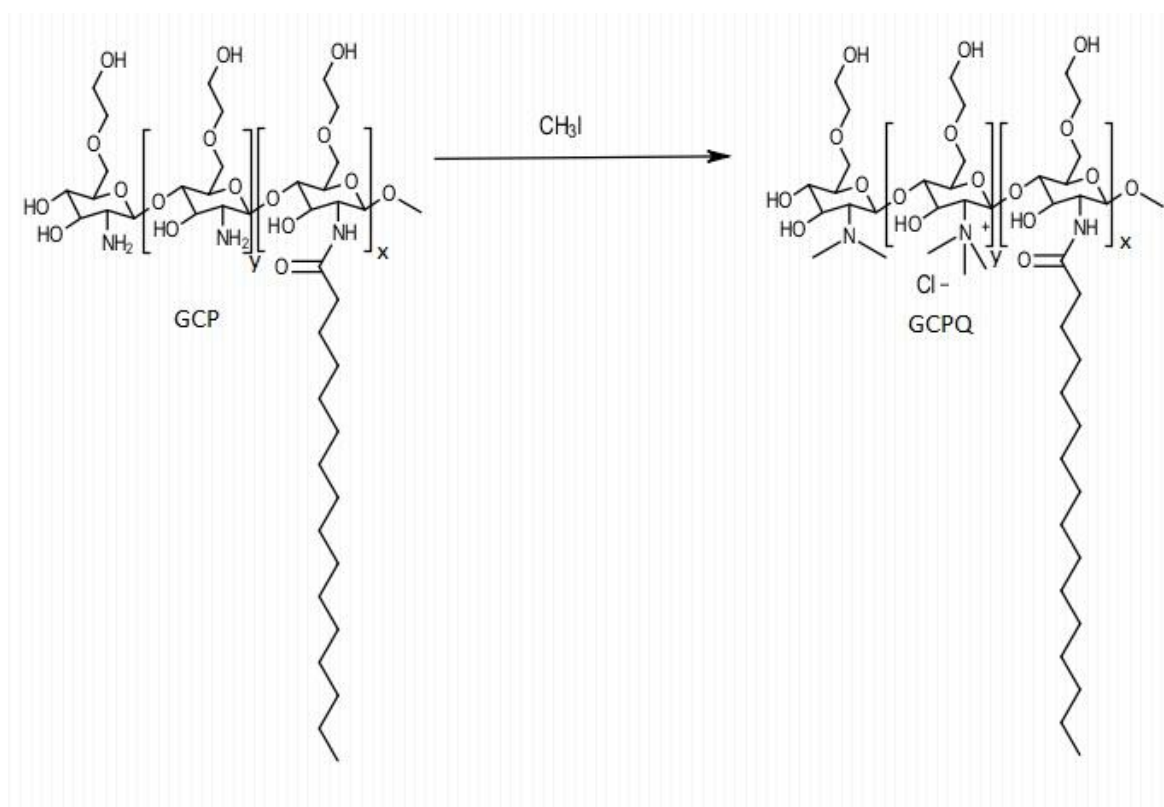


Figure 10: Quaternization of pGC.

### 3.5.3. Iodine removal

To remove iodine from the polymer we used anion exchange method by applying the Amberlite 410(6g of Ambelite 410 per 1g of pGC) which was added to dialysate and stirred for 15 min. Sodium nitrite test was used to check if iodine was successfully removed. Iodide is oxidised with sodium nitrite to iodine which is detected with chloroform (purple solution). After dialysis the polymer solution was first filtered through a filter (porosity 3), by applying vacuum and then snap-frozen and placed into a freeze-drier to dry.

## 3.6. Characterization of GCPQ

### 3.6.1. NMR analysis

To determine the degree of palmitoylation and quaternization and to confirm the identity of the polymer, NMR analysis was carried out. GCPQ was dissolved in deuterated methanol ( $\text{CD}_3\text{OD}$ ) to obtain the 1% w/v concentration of. For calculating the extent of palmitoylation and quaternization two equations were used (*Equation 1* and *Equation 2*).

The degree of palmitoylation ratio, i.e. the quotient of palmitoyl methyl protons to sugar skeleton protons was calculated by *Equation 1* and the degree of quaternization ratio, i.e. the quotient of quaternary ammonium methyl protons to sugar unit protons by *Equation 2*.

Equation 1:

$$\% \text{ of Palmitation} = \frac{\text{area of CH}_3 \text{ signal/number of H in CH}_3}{\text{area of sugar chain/number of H in sugar skeleton}}$$

Equation 2:

$$\% \text{ of Quaterization} = \frac{\text{area of quaterized ammonium signal/number of H in N(CH}_3)_3}{\text{area of sugar chain/number of H in sugar skeleton}}$$

In the GCPQ <sup>1</sup>H-NMR spectrum five main signals should be observed, which define the polymer. At around 0.9 ppm methyl end of palmitic acid chain was present. The peak between 1.2 and 1.4 ppm confirmed the presence of the palmitic acid chain. The CH<sub>2</sub> of the palmitic acid, next to the C=O group appeared at 2.4 ppm. The quaternized ammonium produced area peak at 3.4 ppm. At 3.5 - 4.5 ppm the peak of sugar skeleton was located, while the solvent peak was present at 3.3 ppm.

### 3.6.2. GCP MALLS analysis

Furthermore, molecular weight of the synthesised polymer was determined by GPC MALLS analysis.

To measure molecular weight (M<sub>w</sub> and M<sub>n</sub>) and polydispersity index (PDI) of the GCPQ synthesised polymer, Gel permeation chromatography together with Multi Angle Laser Light Scattering (GPC MALLS) was used.

The GPC-Malls system used was equipped with: Dawn Heleos II MALLS detector (120 mW solid-state laser operating at 658 nm), Optilab rEX interferometric refractometer (flow cell: 7.4 μL at 658 nm), quasi elastic light scattering (QELS) detectors (Wyatt Technology Corporation, Santa Barbara, CA, USA), Agilent 1200 autosampler (Agilent Technologies, UK) and POLYSEP-GFC-P guard column (35 x 7.8 mm, Phenomenex, Macclesfield, U.K.), attached to a POLYSEP-GFC-P 4000 column (300 x 7.8 mm, Phenomenex).

The measurement was performed at room temperature with a mobile phase flow rate of 0.7 mL/min. The results were analysed using ASTRA software (Wyatt Technology Corporation) for Windows system, version 5.3.4.

The GCPQ polymer was dissolved in the mobile phase, to obtain the concentration of 5 mg/mL. All samples were filtered through 0.22 µm syringe filter to remove bigger particles. For the specific refractive index ( $dn/dc$ ) of GCPQ, the same mobile phase was used as for analysis of sample. Six samples containing 0.1 to 0.6 mg of GCPQ/mL were prepared and filtered through 0.22 µm syringe filters, and then manually injected from the lowest to the highest concentration, starting with the mobile phase as a blank. The measured refractive indices were used to calculate the molecular weight of GCPQ.

The mobile phase used was a mixture of 500 mM acetate buffer (0.3 M anhydrous sodium acetate, 0.2 M glacial acetic acid, pH = 4.5) and methanol (35:65 v/v).

### 3.7. Calibration curve for CsA

To be able to determine the exact content/concentration of CsA in our formulation, we created a calibration curve by using its standard solutions in methanol, starting with 1.25 mg/mL, down to 0.01 mg/mL.

#### 3.7.1. HPLC analysis of CsA

We used the following HPLC protocol for measuring the quantities of CsA in our formulations following the homogenization process and also during the stability study.

Samples were analysed using analytic reverse-phase HPLC. They were chromatographed over the Onyx™ Monolithic C18, LC Column (100 x 4.6 mm), using water and acetonitrile (60:40) mobile phase, driven by the Agilent Technologies 1200 series HPLC system, at a flow rate of 1.5 mL min<sup>-1</sup>. The column was maintained at 40 °C. For CsA separation gradient mobile phase was used (Table III), and the analyte was detected with the UV-VIS detector at 210 nm.

Table III: Mobile phase gradients, used for CsA HPLC analysis.

Time [min]	Water [%]	Acetonitrile [%]
0	60	40
4	5	95
5	5	95
7	5	95
7.5	60	40
9.5	60	40

### 3.8. Improving solubility of CsA before homogenization to achieve its higher encapsulation yields

With greater drug solubility, the process of its encapsulation is more efficient because less amount of it precipitates when injected into homogenizer. When we mixed CsA with GCPQ solution, most of the drug precipitated on its surface. After dispersing it by vortexing CsA distributed equally within the solution, but only for few seconds, and then precipitated again on the surface. As CsA has better solubility at low temperatures, we placed the samples in a cold room (4 °C) and stirred them with magnetic stirrer (37). Then 200µL aliquots were collected from each sample at 0, 1, 3, 5 and 21 hours. We took them from the middle of each solution, just few seconds after stirring was stopped, so that the not solubilized drug could float on the surface. The samples taken at each time point after dispersing were photographed.

All collected samples were analysed by HPLC determine the amounts of CsA they contained.

### 3.9.Reducing the number of homogenization cycles

The number of homogenization cycles determined the size and uniformity of particles in our formulations. To find out how many are actually needed, we performed an experiment, where the tested formulations were analysed following different numbers of homogenization cycles. Samples were collected before homogenization and after 0, 1, 2, 3, 5, 10 15, 20, 25, 30 and 35 cycles. They were kept in fridge for 2 - 3 hours before being

analysed with the ZetaSizer NS apparatus, using DLS (Dynamic Light Scattering) technique, as detailed above. The formulation contained 3.0% glycerol in water, 0.75% GCPQ (DP = 31%, DQ = 16%) and 0,02% CsA. For each condition tested, three replicates were homogenized and analysed.

### 3.10. Production of eye drops

Appropriate amount of GCPQ was weighted into vials to get 0.75% w/v concentration in a solution containing 2,7% glycerol in water. The polymer was completely dispersed by gently shaking the solution for at least 2 h. The polymer solution was added to a desired amount of CsA powder (twice as much as the target quantity). The drug was dispersed first by vortexing the mixture and then by stirring it with magnetic stirrer at 4 °C, for 3 - 5h.

#### 3.10.1. High pressure homogenization

After a desired amount of CsA was added to the GCPQ dispersion the Avestin C5 High Pressure Homogenizer (Figure 11) was used for to encapsulate it into nanoparticles. The dispersion was first transferred into 20 mL syringes and then the homogenization process was carried out in a fume hood. The formulation was cycled 10 - 15 times at 17.000-19.000 psi. After the homogenization process was completed the tested formulations were transferred into glass vials and their pH values were adjusted with 1M NaOH, as follows.



Figure 11: Avestin C5 homogenizer (38).

### 3.10.2. pH value adjustment

pH value of tested formulations was adjusted to 7.0 with 1M sodium hydroxide (NaOH). For this purpose direct titration using pH meter and magnetic stirrer was carried out.

After pH adjustment the samples were placed in a fridge for at least 24 h, so that the solubility of CsA increased. The next day HPLC analysis was carried out. Samples were first diluted with an equal volume of methanol and then chromatographed, as described above, and analysed against the CsA calibration curve.

Formulations were then diluted with 0.75% w/v GCPQ dispersion in 2.7% glycerol solution in water to desired concentrations of CsA and filtered through 0.22  $\mu\text{m}$  syringe filters directly into 3 mL plastic sterile containers (Steri-Dropper™ Polyethylene Sterile Eye-Dropper Bottles). Both procedures were carried out in a sterile environment of low air flow hood.



Figure 12: Steri-Dropper™ Polyethylene Sterile Eye-Dropper Bottles.

### 3.11. Stability test

We have prepared sterile eye drops with three different concentrations of CsA, i.e. 0.01%, 0.02% and 0.05%, each in three replicates, which were then stored in three different environments at different temperatures: fridge at 5 – 6 °C, room temperature (18 – 25 °C) and incubator at 40 °C. We tested the following five stability parameters: concentration of CsA, osmolarity, viscosity, zeta-potential and particle sizes. All formulations were also observed visually for any changes. All measurements were made at days 0, 7, 14, 21 and 28.

### 3.11.1. CsA concentration

Drug concentrations were measured using the HPLC method, as described above.

### 3.11.2. Osmolarity

Roebing MICRO-Osmometer Type 5R was used to determine osmolarity of samples. This is a manual osmometer that uses freezing point depression in comparison to pure water. To ensure that the instrument was performing properly, we used standard, i.e. 0.9% sodium chloride solution against double distilled water. The samples (100  $\mu$ L each) were pipetted into 1.5 mL Eppendorf tubes and measured with freezing point depression technique.

### 3.11.3. Viscosity

The M-VRoc<sup>TM</sup> Viscometer was used for measuring viscosity. Samples were inserted in the measuring cell using 0.5mL syringe. Viscosity was measured at three different high shear rates, at 20 °C: approx. 10.700 s<sup>-1</sup>, 12.500 s<sup>-1</sup> and 14.300 s<sup>-1</sup>. The samples were considered to be Newtonian fluid because of low concentration of polymer used (7.5%) (39).

### 3.11.4. Zeta potential and particle size

Zeta potential (ZP) and particle sizes were measured at 25 °C, using Malvern ZetaSizer Nano SZ instrument. For ZP measurements and for size measurements 40 $\mu$ L disposable cuvettes were used.

## 3.12. The GCPQ assay

Samples were chromatographed over Waters Acquity BEH Amide, 50 x 2.1mm, 1.7 $\mu$ m UPCL column, using isopropyl alcohol and 70:30 (v/v) mixture of Milli-Q Water : Acetonitrile plus 0.2% Formic Acid (90:10) as a mobile phase, which was driven by the Agilent Technologies 1600 series HPLC system, at a flow rate of 0.3 mL min<sup>-1</sup>. The column was kept at 35 °C. GCPQ was detected with Agilent ELSD detector using nebulizing temperature of 70 °C, evaporation temperature 60 °C and N<sub>2</sub> flow of 1.6 L min<sup>-1</sup>. For GCPQ separation gradient mobile phase over 15 min run with 5 min post run (Table IV) was applied.

Table IV: Gradient mobile phase for GCPW assay.

Time [min]	Isopropil alcohol	70:30 (v/v) Milli-Q Water:Acetonitrile + 0.2% formic acid
0	90	10
7	0	100
14	90	10

Samples used for creation of calibration curve were prepared in methanol with concentrations of 0,25; 0,50; 0,75; 1,0 and 1,5 mg mL<sup>-1</sup>. Samples of our formulations were diluted 10 times with methanol and chromatographed.

### 3.13. Sterility test

The sterility test was performed according to the United States Pharmacopeia (USP 39, 2016 <71> STERILITY TEST). However we had to modify the test, because we did not have all prescribed microorganisms available (*Clostridium sporogenes*, *Candida albicans* and *Aspergillus brasiliensis*).

Sterility was tested with the following microorganisms: *Staphylococcus aureus* (NCTC 12923), *Bacillus subtilis* (NCTC 8236) and *Pseudomonas aeruginosa* (ATCC 10662) in aerobic, and *Escherichia coli* (NCTC 10419) in anaerobic conditions instead of *Clostridium sporogenes*.

All stated bacteria were grown in tryptone soya broth (TSB) media. We used direct inoculation technique. All inoculations were performed in sterile environment. For growth promotion test the inoculum of 50 colony forming units (CFUs) of each bacterium was added to 14 mL of TSB. For the method suitability test, 1 mL of formulation tested and the inoculum of 50 CFUs of each microorganism were added to 14 mL of TSB. The tubes were then incubated for 3 days at 37 °C. Those containing *E. coli* were kept in anaerobic conditions (Microbiology Anaerocult®, Merck, Germany).

Only formulations containing 0.02% CsA were used for sterility testing and each test was carried out in triplicate. To 14 mL of TSB 1 mL of each formulation sample was added. We also prepared two negative controls, one with 1 mL of sterile water and one just with

TSB. The tubes were incubated for 14 days at 37 °C. Unfortunately we could not determine the growth of bacteria in tubes containing formulation samples, because TSB became turbid immediately after it was mixed with formulation. Therefore, to be able to determine bacterial growth, plates with TSB agar were inoculated with liquid TSB (2 µL) taken from each sample containing tubes. The plates were then incubated for 3 days at 37 °C.

## 4. RESULTS AND DISCUSSION

### 4.1. Synthesis of GCPQ

Degradation reaction yield:

$$\frac{\text{Mass of product after degradation}}{\text{Weighted mass of glycol chitosan}} = \frac{23,1g}{25,0g} \times 100\% = \mathbf{92,4\%}$$

Palmitoylation reaction yield:

*Theoretical pGC mass [g]*

$$\begin{aligned} &= \frac{\text{Mass of dGC}}{242,68g/mol} \times \left( \frac{DP\%}{100} \times 446,63 \frac{g}{mol} + \frac{100 - DP\%}{100} \times 205,21 \right) \\ &= \frac{10,2}{242,68g/mol} \times \left( \frac{31,7}{100} \times 446,63 \frac{g}{mol} + \frac{100 - 31,7}{100} \times 205,21 \right) \\ &= 11,8g \end{aligned}$$

$$\frac{\text{Mass of pGC from reaction}}{\text{Theoretical pGC mass}} \times 100\% = \frac{11,1g}{11,8g} \times 100\% = \mathbf{94,1\%}$$

Quaternization reaction yield:

$$\frac{\text{Mass of dry product (GCPQ)}}{\text{Mass of starting material (pGC)}} \times 100\% = \frac{10,2g}{12,1g} \times 100\% = \mathbf{84,3\%}$$

#### 4.1.1. GCPQ NMR analysis

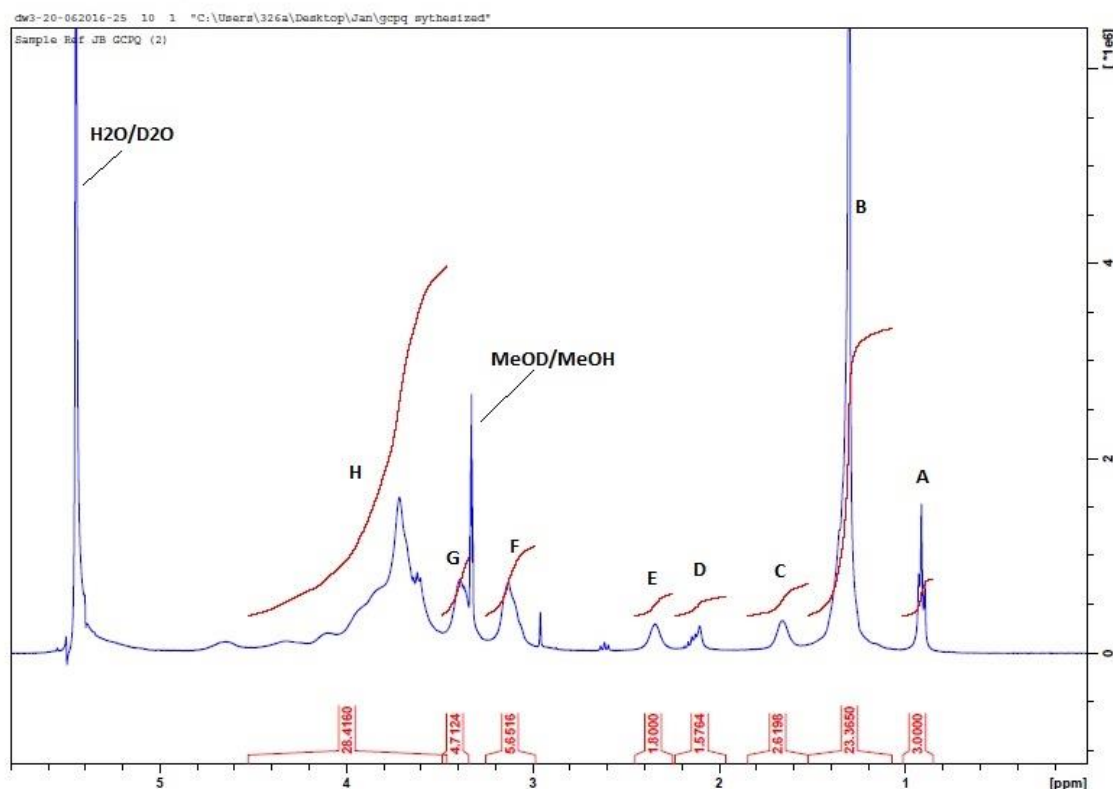


Figure 13: The results of GCPQ NMR analysis: A – CH<sub>3</sub> end of palmitic acid chain, B – palmitic acid chain, C – the second CH<sub>2</sub> in palmitic acid chain, D – acetyl peak, E – the first CH<sub>2</sub> in palmitic acid chain, F – tertiary and secondary amine, G – quaternary amine and H – the sugar backbone.

Characteristics of synthesized GCPQ polymer:

	Mn [Da]	Mw [Da]	PDI	DP%	DQ%
GCPQ	13.640	13.710	1,010	31,7	16,5

#### 4.2. CsA calibration curve

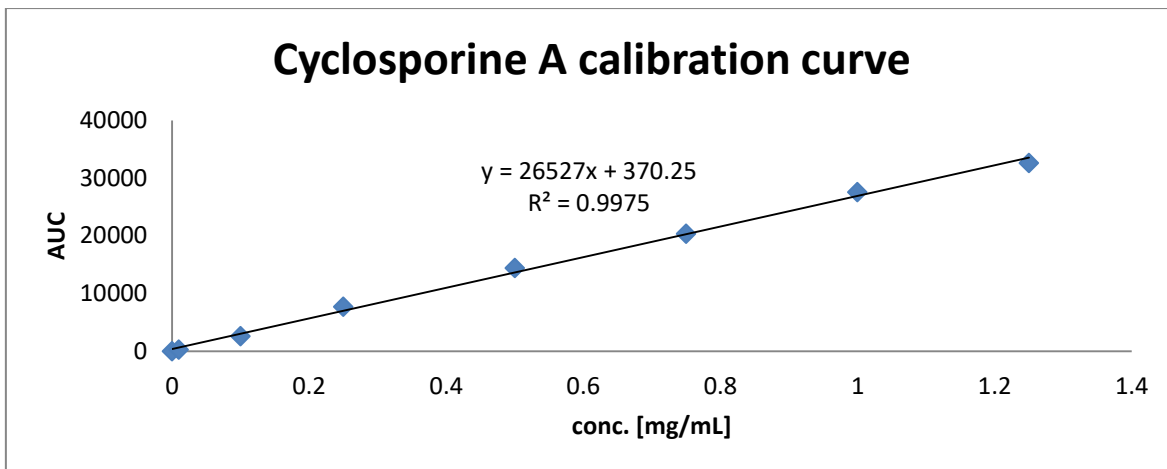


Figure 14: Linearity of the CsA calibration curve.

#### 4.3. Quantification of CsA with HPLC

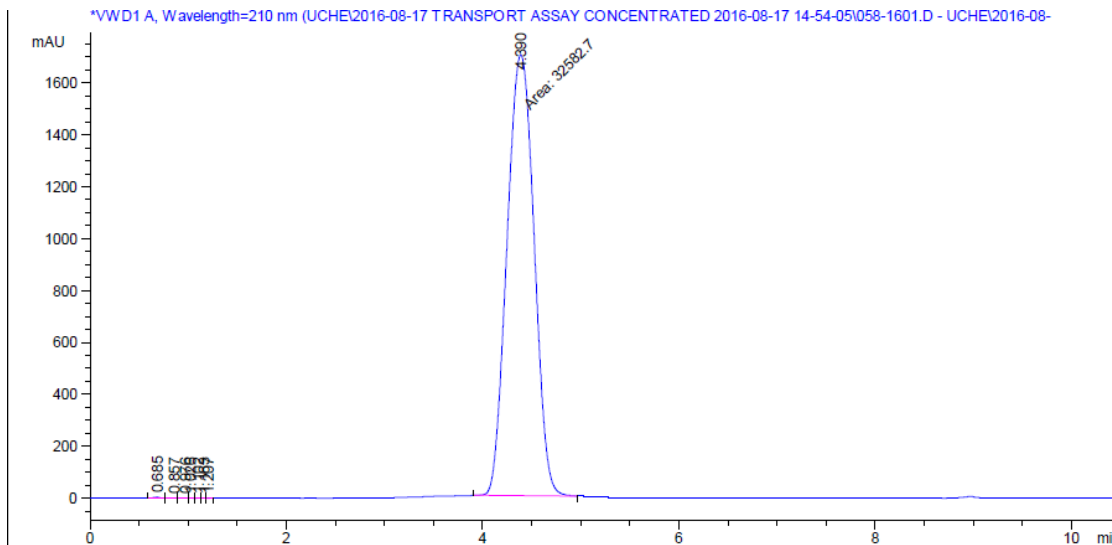


Figure 15: An example of HPLC chromatogram showing a well-defined CsA peak ( $c = 1,25$  mg/mL).

All concentrations of CsA in formulations tested were calculated using the next formula:

$$\text{Conc. in formulation} \left[ \frac{\text{mg}}{\text{mL}} \right] = \frac{\text{AUC of CsA in formulation} - 370,25}{26527} \times 2$$

Table V: Calculated concentrations of 0,01 mg/mL formulations.

0.01 mg/mL samples at 5-6°C						
Day	Sample	1		2		3
	AUC	Conc. [mg/mL]	AUC	Conc. [mg/mL]	AUC	Conc. [mg/mL]
0	1625	0,095	1614	0,094	1609	0,093
7	1588,9	0,092	1714,4	0,101	1607	0,093
14	1686,1	0,099	1673,5	0,098	1600,7	0,093
21	1654	0,097	1678	0,099	1642	0,096
28	1677,4	0,099	1731,9	0,103	1561,6	0,090
0.01 mg/mL samples at 18-23°C						
Day	Sample	1		2		3
	AUC	Conc. [mg/mL]	AUC	Conc. [mg/mL]	AUC	Conc. [mg/mL]
0	1625	0,095	1614	0,094	1609	0,093
7	1651,6	0,097	1640,8	0,096	1604	0,093
14	1652,7	0,097	1682	0,099	1633,1	0,095
21	1699,8	0,100	1702,1	0,100	1634,5	0,095
28	1691	0,100	1731,9	0,103	1647,4	0,096
0.01 mg/mL samples at 40°C						
Day	Sample	1		2		3
	AUC	Conc. [mg/mL]	AUC	Conc. [mg/mL]	AUC	Conc. [mg/mL]
0	1625	0,095	1614	0,094	1609	0,093
7	1648	0,096	1759,2	0,105	1645,5	0,096
14	1676,6	0,098	1728,4	0,102	1602,8	0,093
21	1745,9	0,104	1717	0,102	1612,7	0,094
28	1764,8	0,105	1720,4	0,102	1646,5	0,096

Table VI: Calculated concentrations of 0,02 mg/mL formulations.

0.02 mg/mL samples at 5-6°C						
Day	Sample	1		2		3
	AUC	Conc. [mg/mL]	AUC	Conc. [mg/mL]	AUC	Conc. [mg/mL]
0	2899,0	0,191	3115	0,207	3081	0,204
7	2791,4	0,183	3191	0,213	3203	0,214
14	2833,1	0,186	3211,3	0,214	3272,6	0,219
21	2846,1	0,187	3192,1	0,213	3191	0,213
28	2833,5	0,186	3152,1	0,210	3145,1	0,209
0.02 mg/mL samples at 18-23°C						
Day	Sample	1		2		3
	AUC	Conc. [mg/mL]	AUC	Conc. [mg/mL]	AUC	Conc. [mg/mL]
0	2899	0,191	3115	0,207	3081	0,204
7	2795,7	0,183	3209,6	0,214	3181	0,212
14	2771,9	0,181	3211,8	0,214	3357,2	0,225
21	2882,4	0,189	3291,9	0,220	3326,8	0,223
28	2912	0,192	3129,1	0,208	3166,7	0,211
0.02 mg/mL samples at 40°C						
Day	Sample	1		2		3
	AUC	Conc. [mg/mL]	AUC	Conc. [mg/mL]	AUC	Conc. [mg/mL]
0	2899	0,191	3115	0,207	3081	0,204

7	2754,1	0,180	3235,2	0,216	3170,3	0,211
14	2880,2	0,189	3300,4	0,221	3420,5	0,230
21	2862,6	0,188	3359,4	0,225	3537,5	0,239
28	3071,8	0,204	3441,2	0,232	3663,4	0,248

Table VII: Calculated concentrations of 0,05 mg/mL formulations.

0.05 mg/mL samples at 5-6°C						
Day	Sample 1		Sample 2		Sample 3	
	AUC	Conc. [mg/mL]	AUC	Conc. [mg/mL]	AUC	Conc. [mg/mL]
0	7195,6	0,515	7154,2	0,511	7067,9	0,505
7	7183,8	0,514	7061,6	0,504	6336,5	0,450
14	7138,9	0,510	7174,3	0,513	6505,1	0,463
21	7214,7	0,516	7210,7	0,516	6517,7	0,463
28	7229,6	0,517	7277,8	0,521	6571,9	0,468
0.05 mg/mL samples at 18-23°C						
Day	Sample 1		Sample 2		Sample 3	
	AUC	Conc. [mg/mL]	AUC	Conc. [mg/mL]	AUC	Conc. [mg/mL]
0	7195,6	0,515	7154,2	0,511	7067,9	0,505
7	7245,8	0,518	7078,7	0,506	6405,9	0,455
14	7112,9	0,508	7102,6	0,508	6551,7	0,466
21	7319,2	0,524	7351,5	0,526	6538,1	0,465
28	7199,9	0,515	7377,1	0,528	6687,5	0,476
0.05 mg/mL samples at 40°C						
Day	Sample 1		Sample 2		Sample 3	
	AUC	Conc. [mg/mL]	AUC	Conc. [mg/mL]	AUC	Conc. [mg/mL]
0	7195,6	0,515	7154,2	0,511	7067,9	0,505
7	7285,4	0,521	7080,4	0,506	6351,4	0,451
14	7300,4	0,522	7624,3	0,547	6668,7	0,475
21	7538,1	0,540	7794,4	0,560	6807,1	0,485
28	7516,3	0,539	7889,7	0,567	6894,3	0,492

#### 4.4. Improving the solubility of CsA before homogenization to achieve its higher encapsulation yields

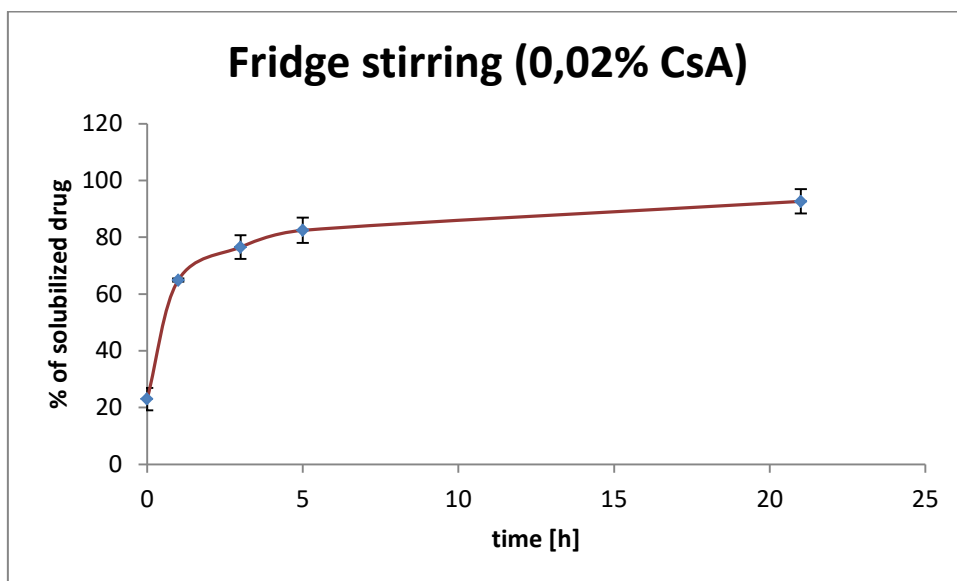


Figure 16: Graph showing the increase of solubilised CsA through time. Samples were incubated at 4 °C and were constantly stirred with magnetic stirrer.



Figure 17: C2 sample - from left to right: 0, 1, 3, 5 and 21 hours of magnetic stirring at 4 °C.

This test was carried out because in first attempts of homogenization we lost a large quantity of drug during the procedure. We analysed the protocol and identified critical points where the probability of drug loss was the highest. The crucial point was the transfer of non-homogenized dispersion with CsA into a syringe for homogenization. As CsA is a hydrophobic molecule with low solubility in water it floated on the surface of dispersion. Vortexing was insufficient in getting the entire amount of drug into the syringe and thus into the homogeniser. We decided to give the drug a bit more time to solubilize in greater extent. Additionally, as CsA has better water solubility at lower temperatures, we placed our formulations into a fridge while being stirred. The results were quite satisfying,

because we saw that in this way formulations containing 0.02% CsA contained more than 80% of the drug within dispersion. Therefore, this step made the process much more efficient, as almost all CsA was retained in formulation after homogenization. Also, as shown in Figure 17 that the amount of visible CsA particles shrink diminished during this step.

#### 4.5. Reduction of the number of homogenization cycles

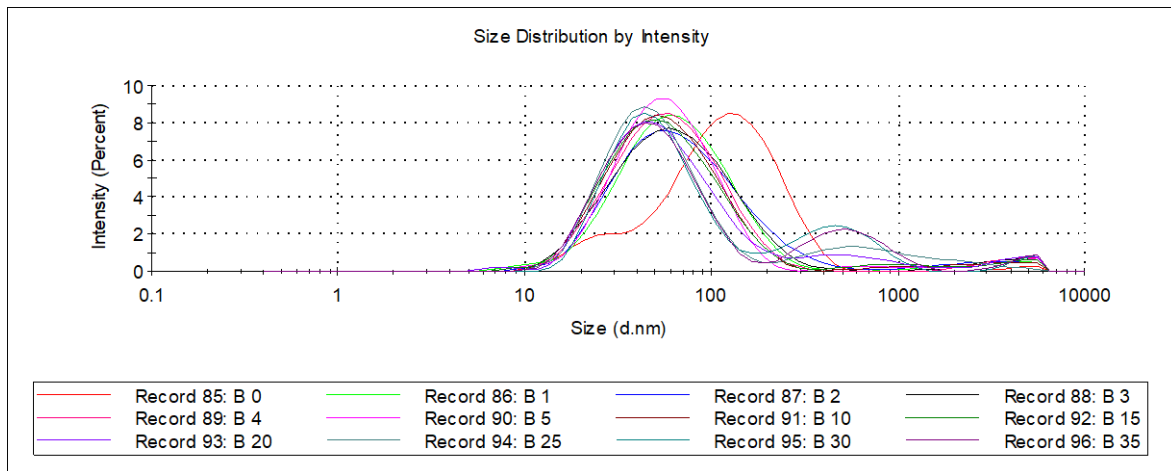


Figure 18: Graph representing distribution of particle sizes in sample A. Red curve represents the non-homogenized formulation. With increasing number of cycles (B0 – B35), a second population of larger particles appears.

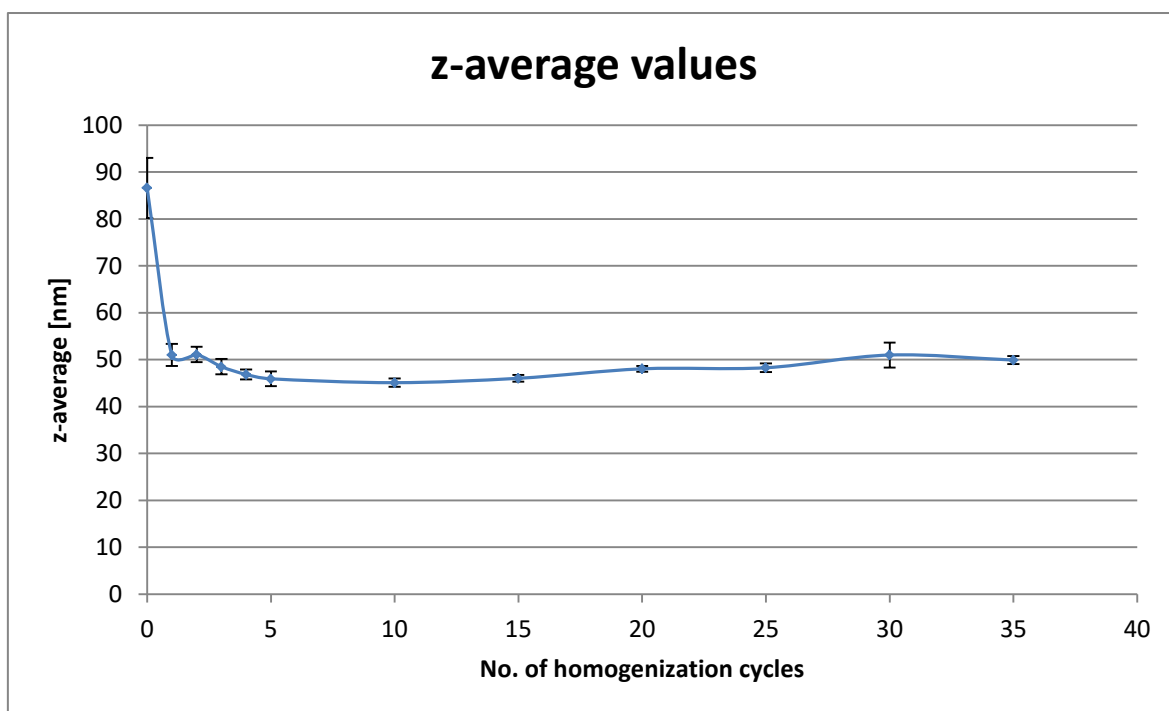


Figure 19: Graphical presentation of z-average values defined in samples of formulation after different numbers of cycles.

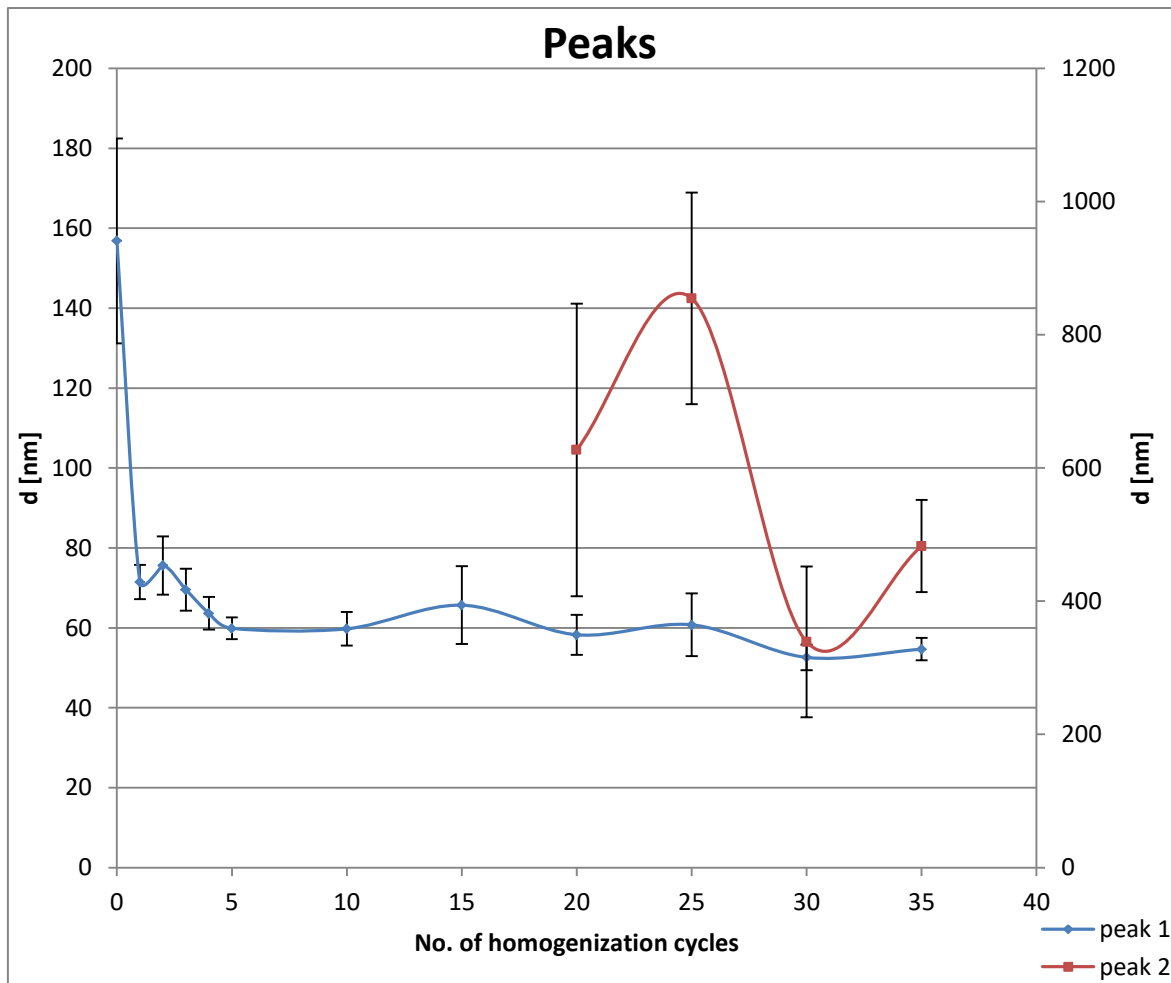


Figure 20: Graph showing us how the peaks change with increasing numbers of homogenization cycles. Blue line represents the population of peak 1 (primary vertical axis) which does not change significantly after 5 - 10 cycles. However after 20 cycles the peak 2 population (secondary axis) appears, which then persists up to the 35<sup>th</sup> cycle.

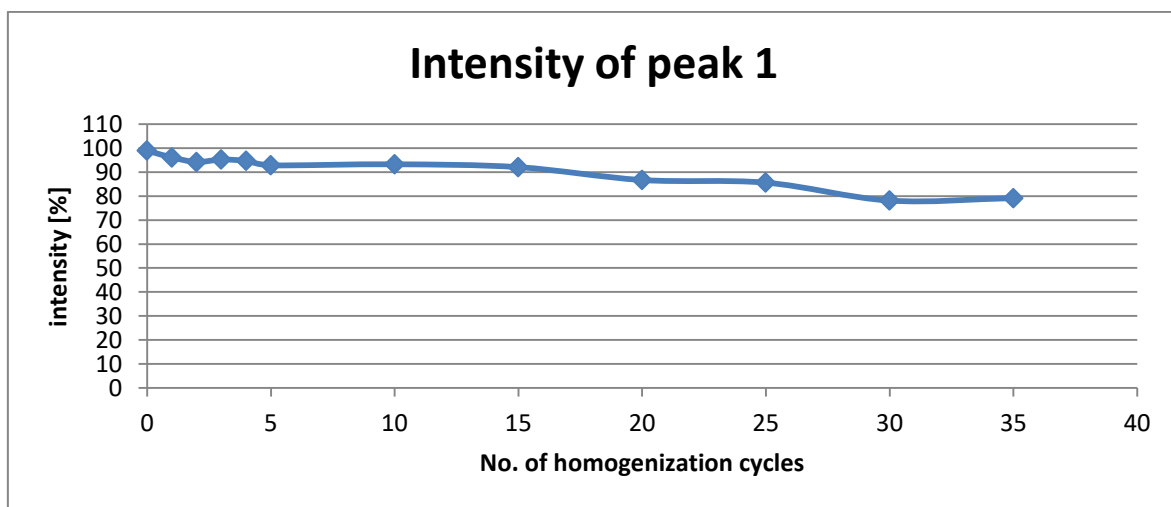


Figure 21: Graphical presentation of DLS signal intensity coming from peak 1 population. The intensity fell under 90% after 15 cycles, when the 2<sup>nd</sup> peak population begins to appear.

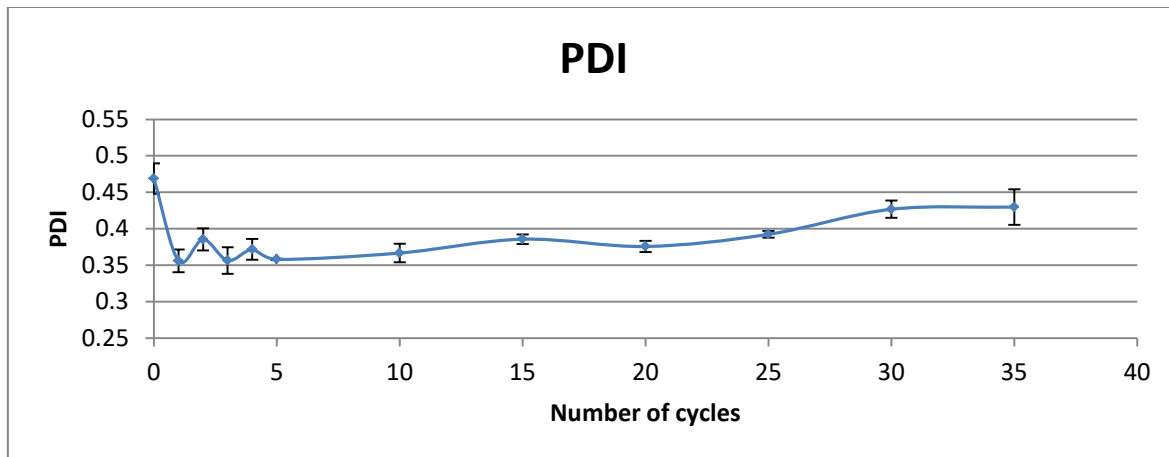


Figure 22: Graph showing the increase of PDI (Polydispersity Index) values with increasing number of cycles, which is a consequence of presence of the second peak population.

After analysing the results of the experiments we decided that 10 – 15 cycles of homogenization are enough to prepare homogenous dispersion with encapsulated CsA. If the number of homogenization cycles was increased, more energy was delivered to dispersed GCPQ particles, which in turn start to aggregate. This might not have any effect on encapsulation efficiency and transport of CsA through eye tissue, however from the economic point of view, less energy and less time to achieve a homogenous dispersion are always welcome.

## 4.6. Formulation stability

### 4.6.1. The GCPQ concentration assay

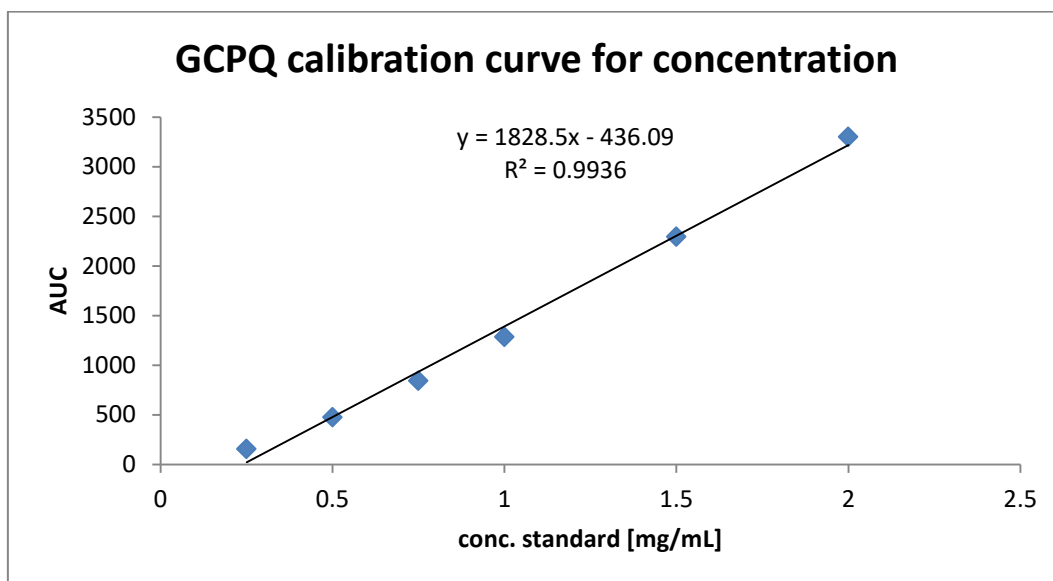


Figure 23: The calibration curve of the GCPQ polymer.

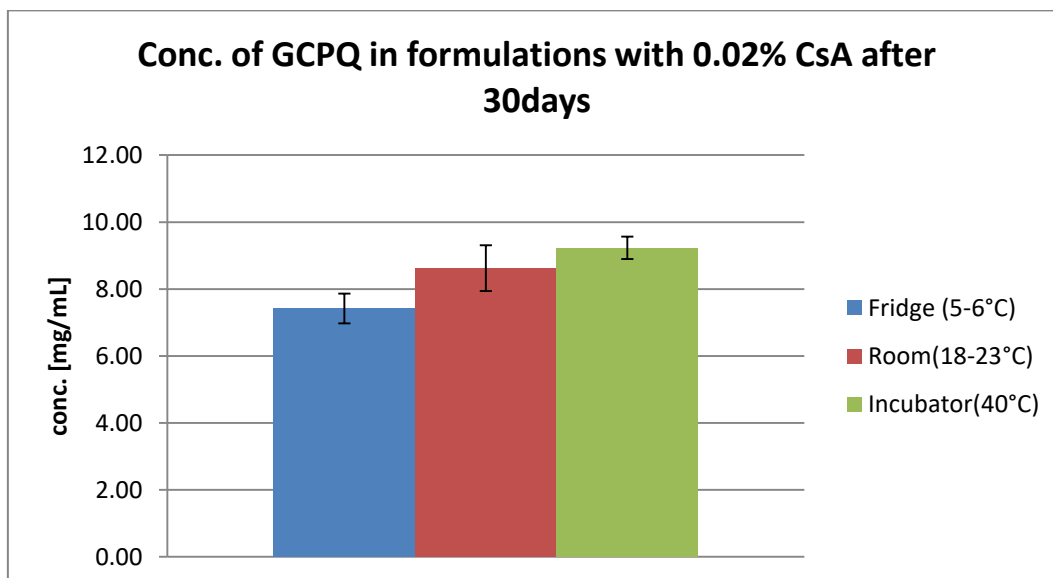


Figure 24: Concentrations of GCPQ polymer in our formulations, after 30 days of their manufacturing, during which time they were kept at different conditions.

Our goal was to prepare formulations containing a 0,75% w/v concentration of nanoparticle forming GCPQ polymer. Eye drops were subjected to many different processes and conditions during their production, until they were finally filtered through

0.22 µm syringe filters and transferred into sterile plastic containers. After the whole production process the concentration of GCPQ polymer has to remain the same. Also, during the 28 days stability testing, some of the polymer could have degraded.

To see if any of the GCPQ polymer was lost or degraded during the production and stability test, HPLC analysis of samples taken from formulations was carried out. We found that that the no polymer was lost or degraded during both processes. A slight rise of GCPQ concentration (Figure 24) in formulations that were stored at room temperature (18 – 23 °C) and in incubator (40 °C) could be ascribed to water evaporation at higher temperatures.

It was also very important that the peaks of all the molecules in our formulations were completely separated. Therefore, the CsA and glycerol peaks must not interfere with the GCPQ peak. Chromatograms presented in Figures 25, 26 and 27, show that with the used HPLC analysis protocol the CsA and the glycerol retention times were under a minute so the separation of the peaks was a success.

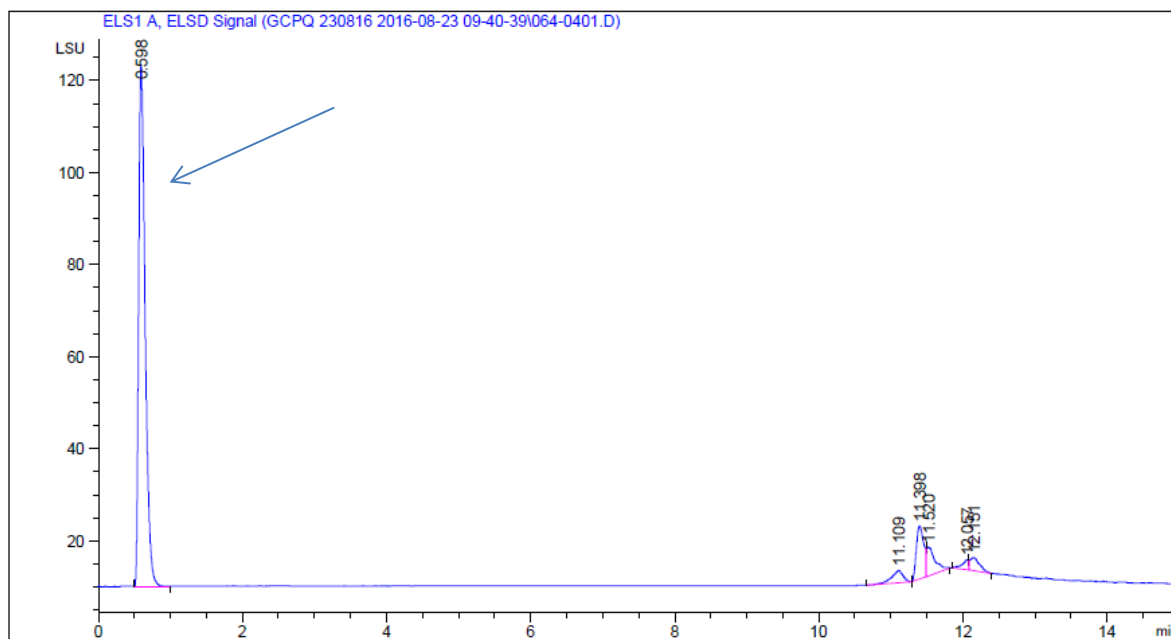


Figure 25: Chromatogram showing the position of the CsA reference peak.

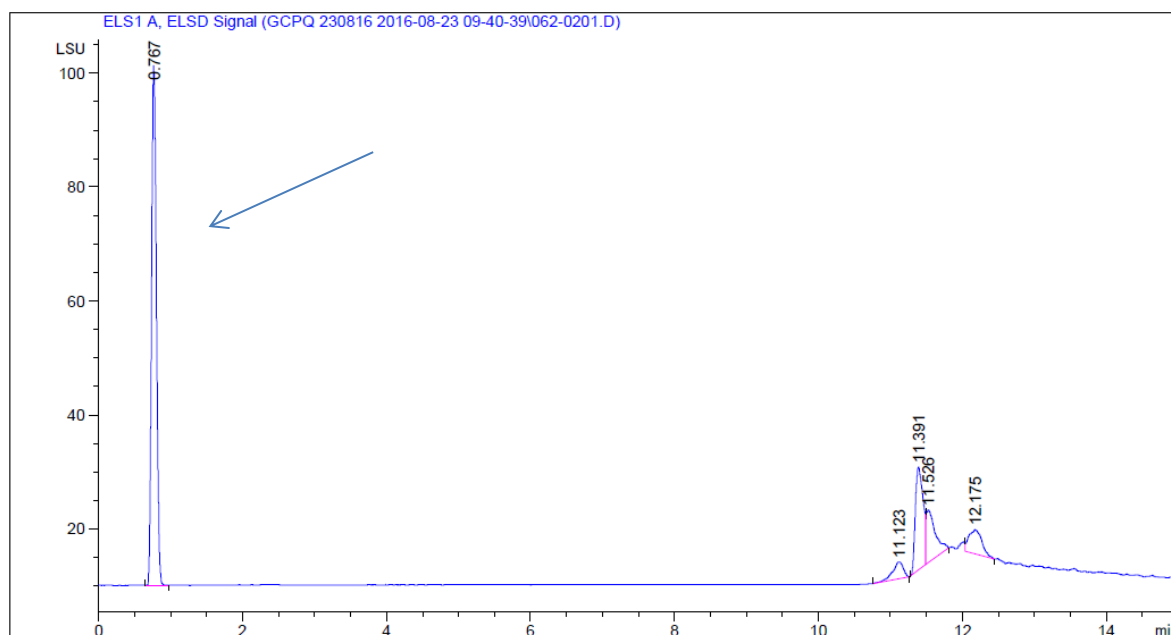


Figure 26: Chromatogram showing the position of the glycerol reference peak.

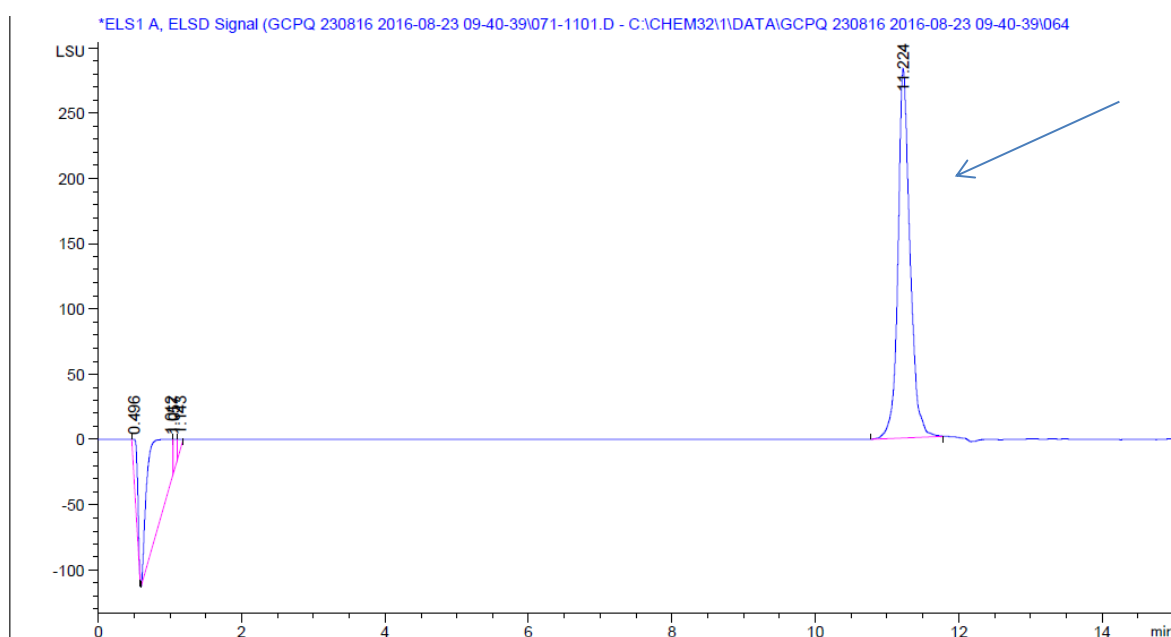


Figure 27: Chromatogram showing the position of the GCPQ peak. The inverted peak in the beginning of the chromatogram is a result of subtracting the blank run (control sample without GCPQ, containing only CsA).

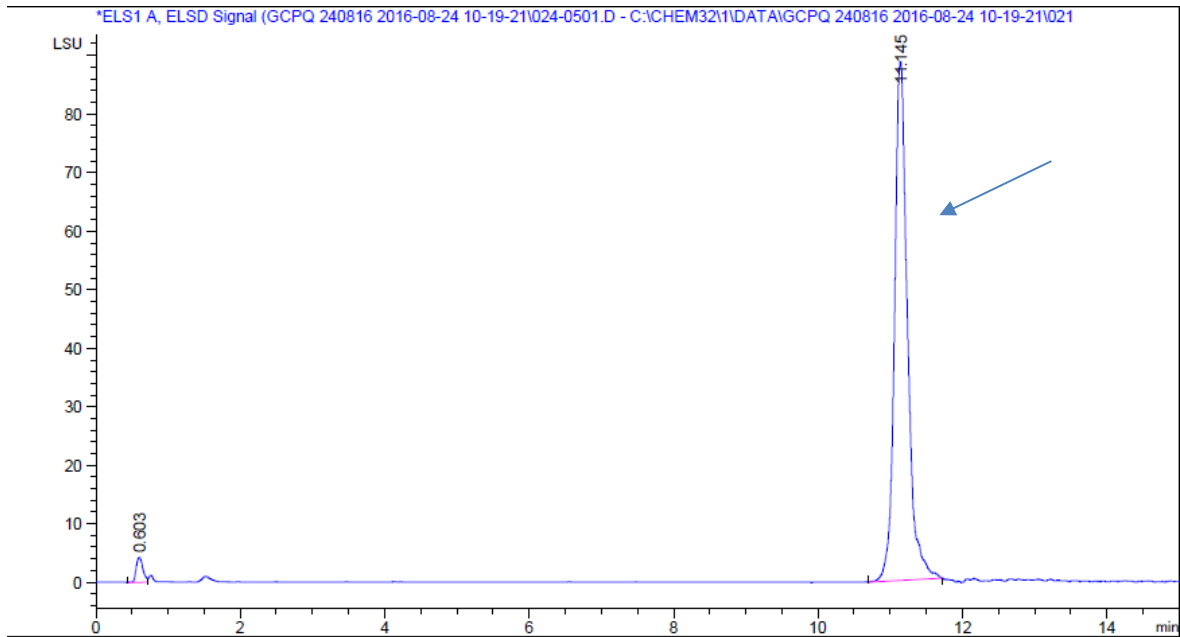


Figure 28: Representative chromatogram of a formulation sample showing the position of the GCPQ peak.

#### 4.6.2. Concentrations of CsA

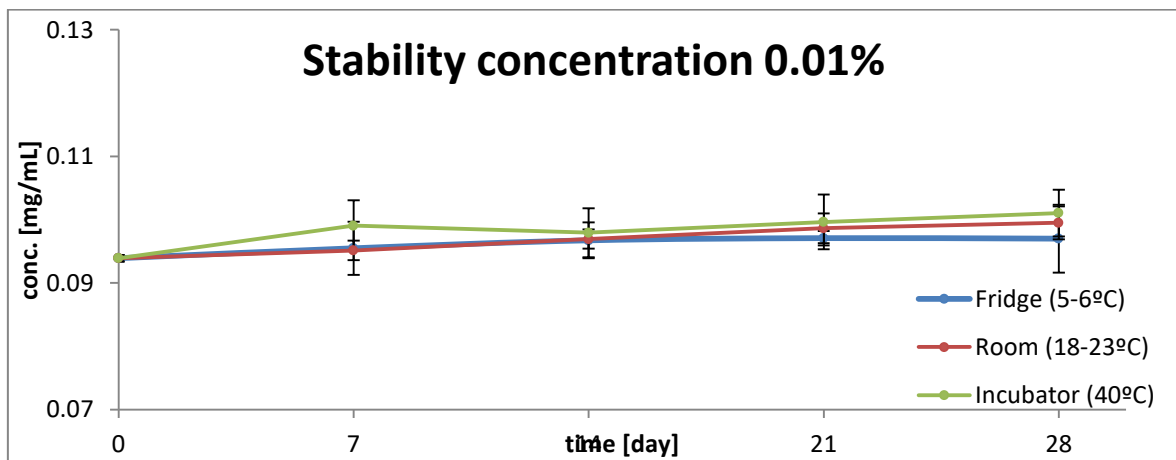


Figure 29: Concentrations of CsA in 0,01% formulations during the course of the stability study carried out under different conditions.

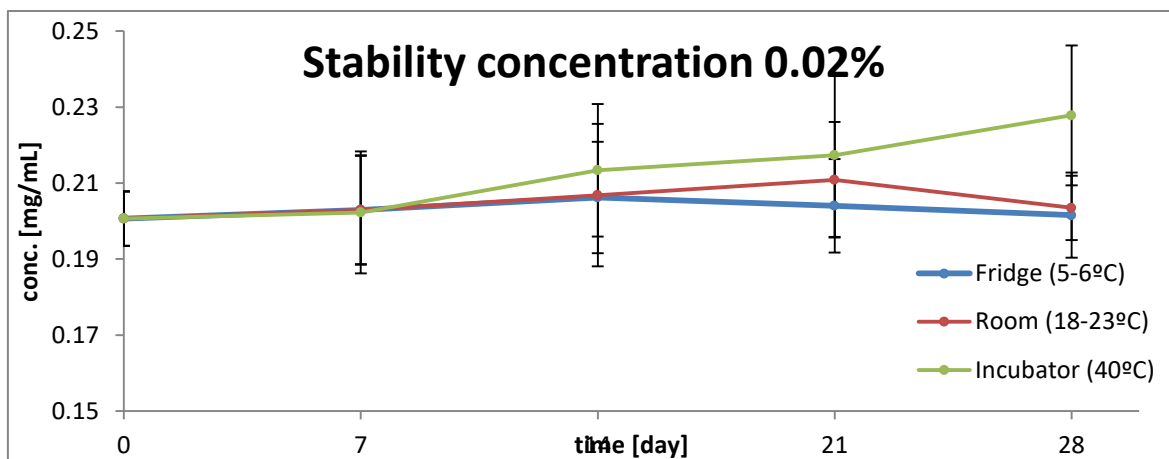


Figure 30: Concentrations of CsA in 0,02% formulations during the course of the stability study carried out under different conditions.

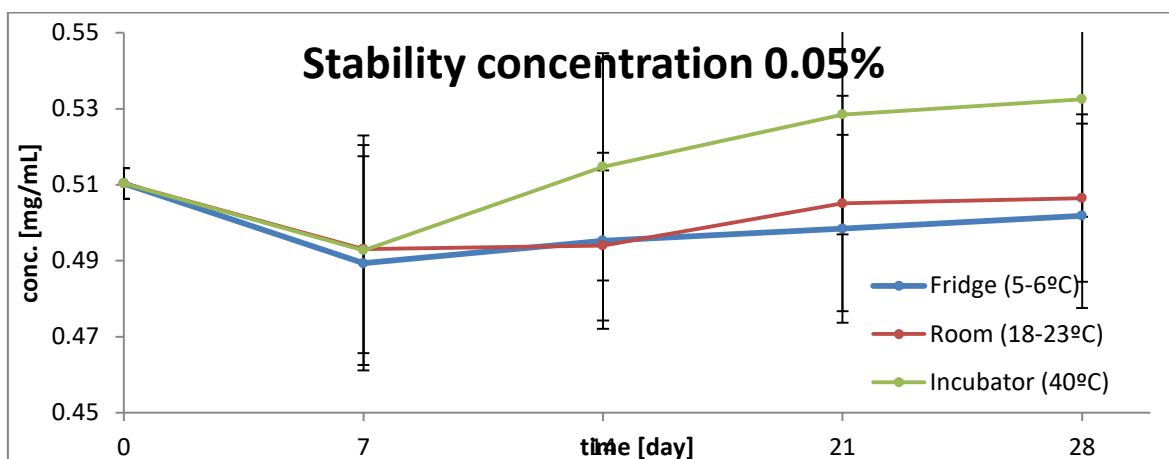


Figure 31: Concentrations of CsA in 0,05% formulations during the course of the stability study carried out under different conditions.

It is crucial that the active drug in a given formulation does not degrade through time. We have proved that during 28 days long stability study CsA in our eye drops has not degraded. So we can claim for the formulations that were stored at room temperature and in fridge, that CsA they contained was stable for the whole period of stability testing. What concerned us a bit, was the rise of its concentration in formulations kept at 40 °C. This could probably be a consequence of water evaporation. Namely, we had to open and close back containers every week, and it might be that they have not been closed properly and water vapours found their way out.

#### 4.6.3. Osmolarity

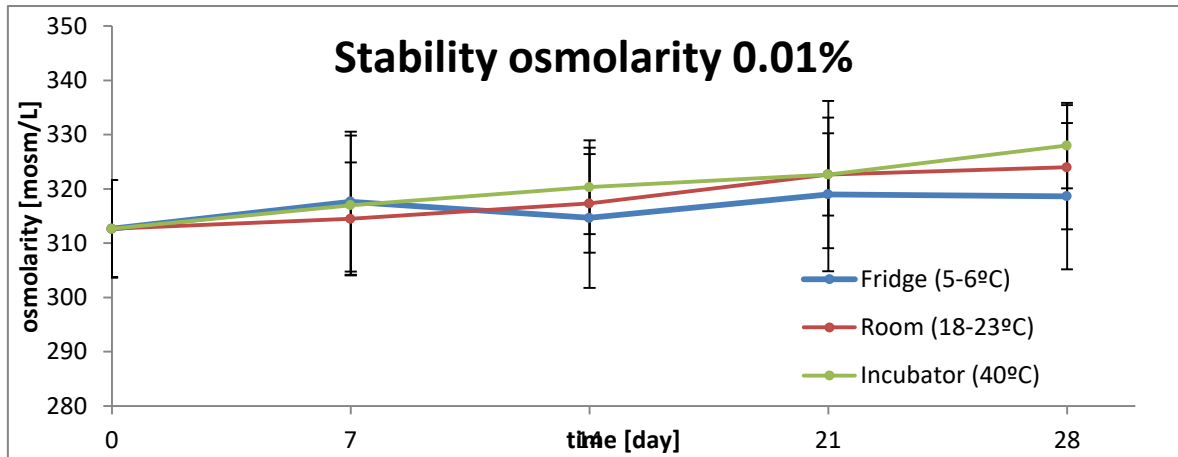


Figure 32: Graph representing the changes of osmolarity in formulations containing 0,01% CsA, during the course of stability study, carried out under different conditions.

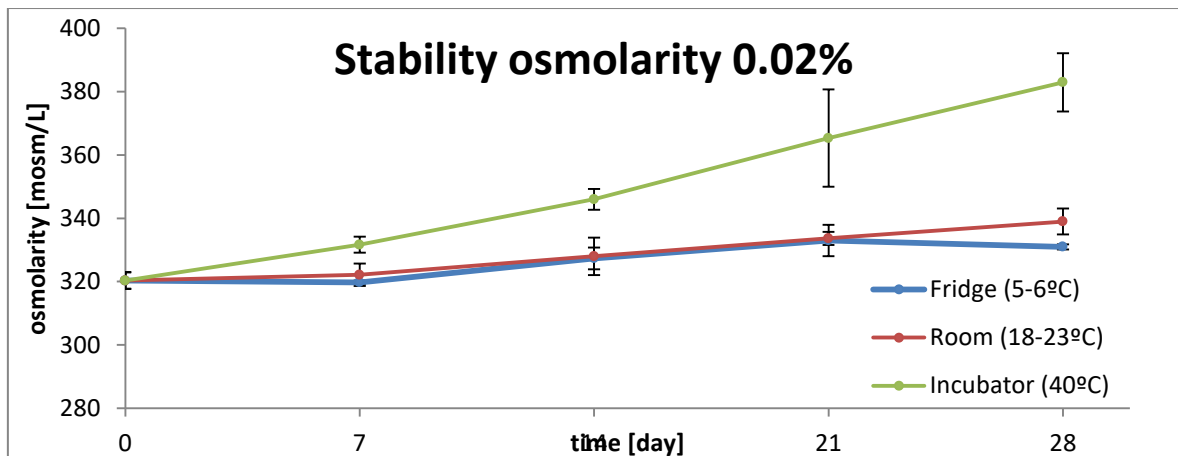


Figure 33: Graph representing the changes of osmolarity in formulations containing 0,02% CsA, during the course of stability study, carried out under different conditions.

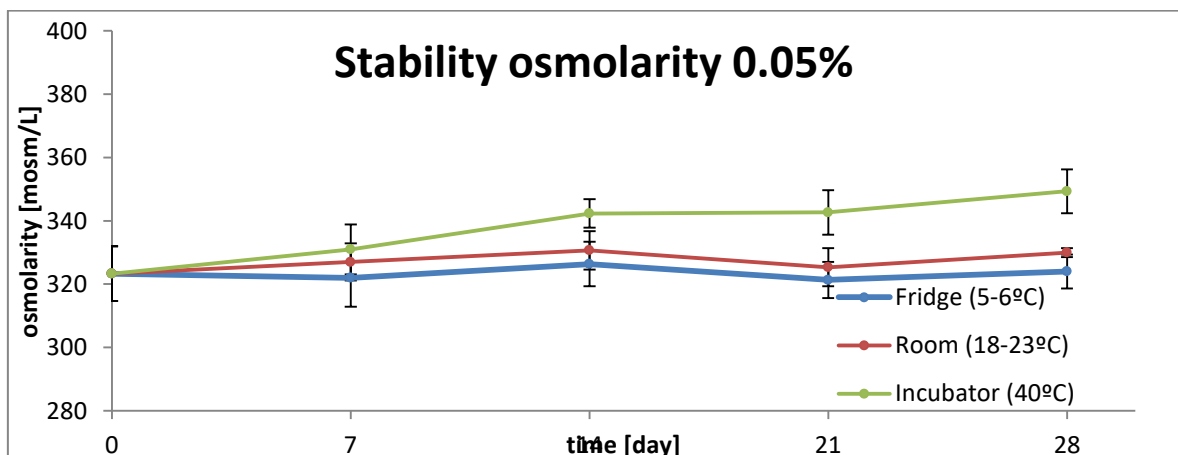


Figure 34: Graph representing the changes of osmolarity in formulations containing 0,05% CsA, during the course of stability study, carried out under different conditions.

Osmolarity was the second parameter measured during our stability test. This parameter has to stay within the physiological range, as it is important that formulations are accepted/tolerated on/in human body. High osmolarity can pull the water out of the cells, or the cells can pull water inside them when osmolarity is too low. Therefore we are always aiming at the osmolarity of 300mosm/L and above, which is the physiological range.

Again, as seen in case of determining CsA concentration, formulations stored in fridge gave good results. Osmolarity of formulations kept at room temperature has risen slightly, probably due to water evaporating out of containers. This effect was again pronounced in formulations that were stored at 40 °C, where due to greater evaporation of water, concentration of glycerol in our formulations increased, which resulted in higher osmolarity.

#### 4.6.4. Viscosity

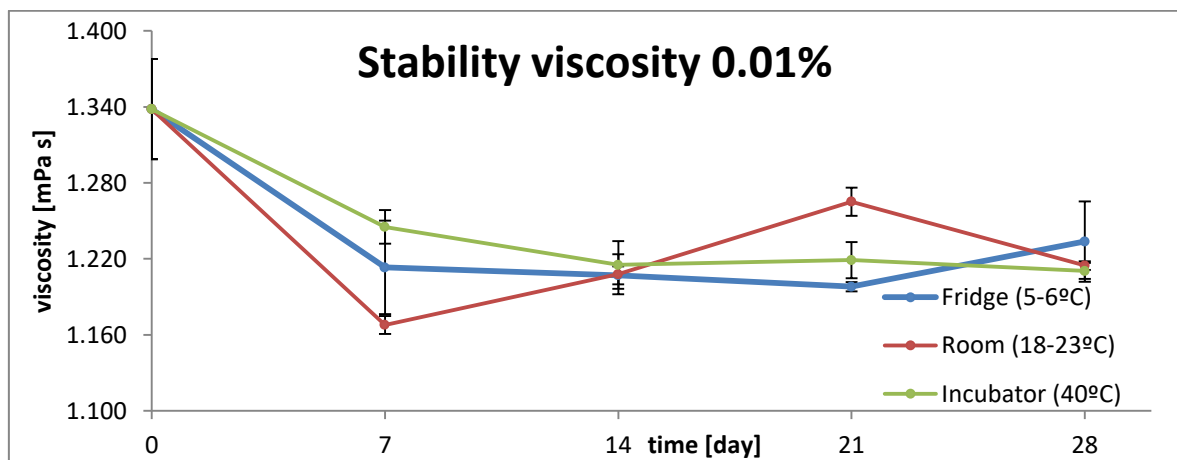


Figure 35: Graph showing changes in viscosity of formulations containing 0,01% CsA during the course of the stability study, carried out under different conditions.

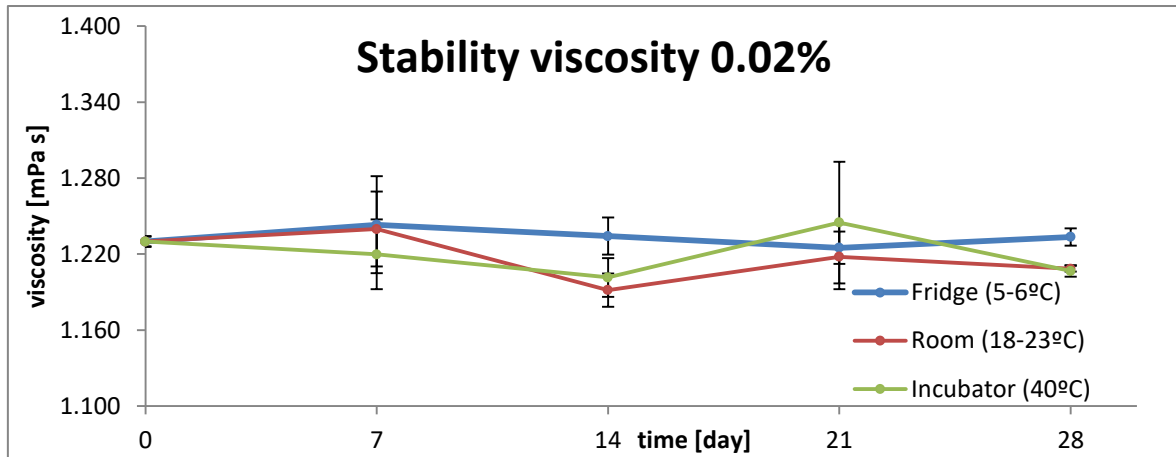


Figure 36: Graph showing changes in viscosity of formulations containing 0,02% CsA during the course of the stability study, carried out under different conditions.

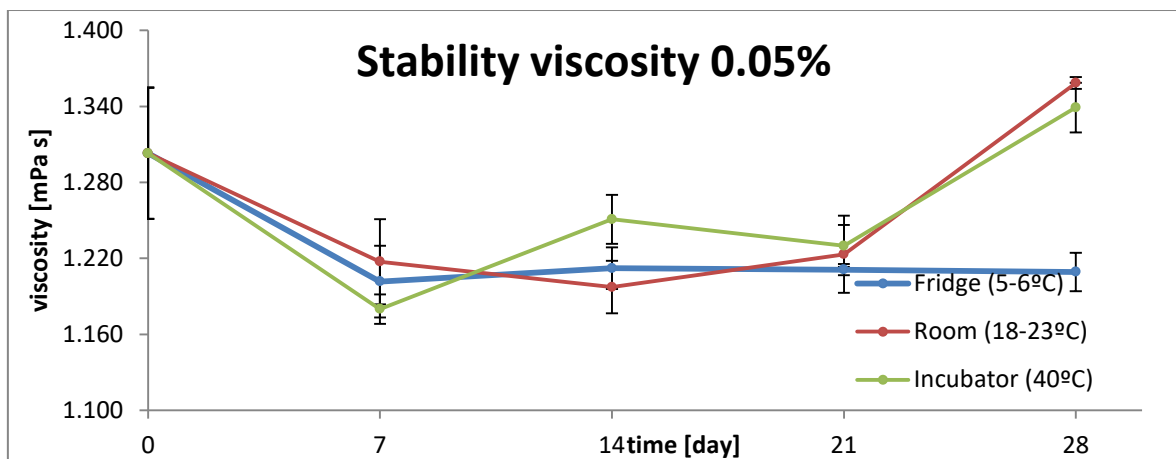


Figure 37: Graph showing changes in viscosity of formulations containing 0,05% CsA during the course of the stability study, carried out under different conditions.

Viscosities of eye formulations should be measured at high shear rates. This is because during blinking high shear rates are generated in tear film. We have considered our formulations as Newtonian fluids because we have only used low concentrations of GCPQ polymer (39).

Graphs in Figures 35, 36 and 37 show some divergences in viscosity values measured at defined time points throughout stability testing. They can be a result of many different factors, such as: the setting of viscosimeter each day a bit differently, transferring samples into measurement cell, and even though we were very careful not to create any air bubbles

in tested samples, there is still possible that some of them were present in junctions, from where they could enter into the measuring cell.

#### 4.6.5. Zeta potential

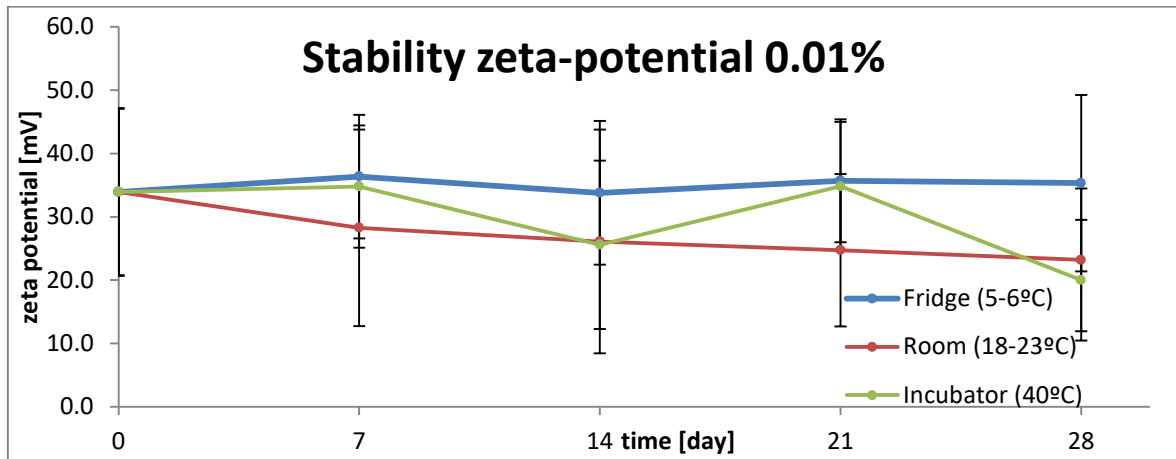


Figure 38: Graph showing changes in zeta potential of formulations containing 0,01% CsA during the course of the stability study, carried out under different conditions.

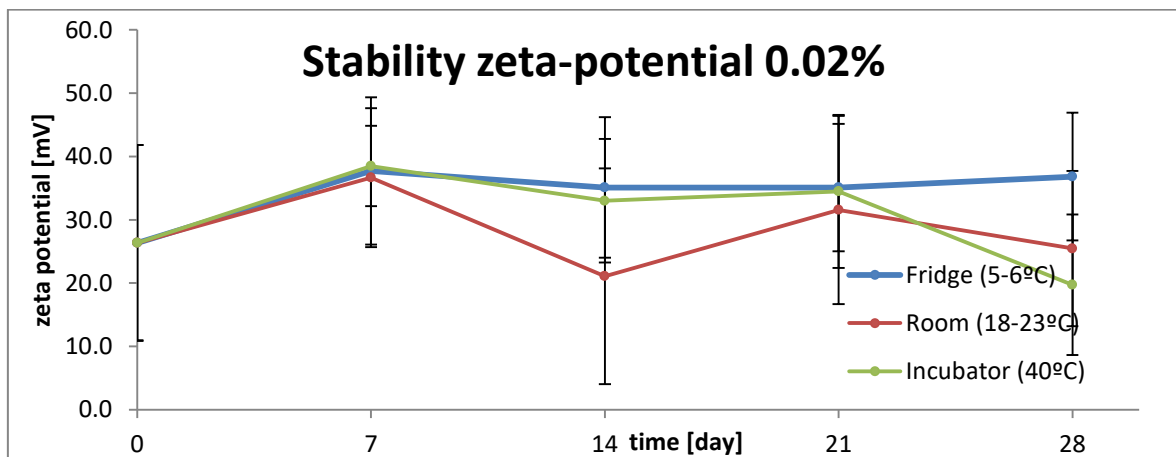


Figure 39: Graph showing changes in zeta potential of formulations containing 0,02% CsA during the course of the stability study, carried out under different conditions.

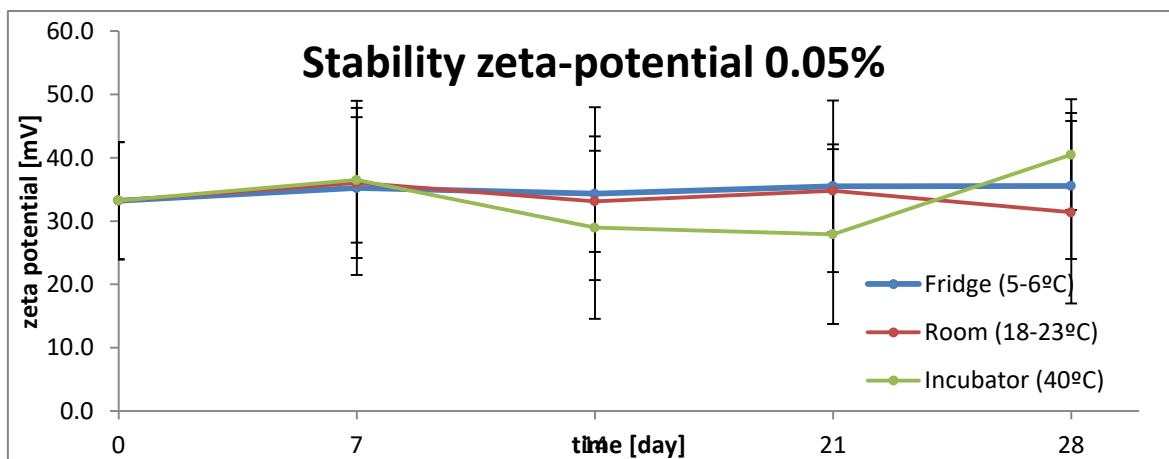


Figure 40: Graph showing changes in zeta potential of formulations containing 0,05% CsA during the course of the stability study, carried out under different conditions.

Zeta potential was the most hard to measure parameter. Our polymer contained a positive charged quaternized nitrogen atom which gave a net positive charge to our formulations. The reason why we did not get better results with lower standard deviation values is probably due to two main factors. The first one is that our formulations were not monodisperse, as they contained more than one size population of particles and second, that they contained particles < 20 nm.

Zeta potential tells us how likely the particles present in a solution will stick together or how stable is a given dispersion. Even though our measurements were not as we were expecting them to be, i.e. with low SD values, we can still conclude that the formulations were stable. We made this claim after we have compared zeta potential values with particle sizes. Namely, the mean zeta potential values in most samples did not change and if we consider particle size distribution graphs at the same time, we see that particle sizes do not change as well.

#### 4.6.6. Particle size

Particles formed two population peaks in our formulations (Figure 41). One peak, which represents the majority of particles, was situated at around 50 nm and the second one at around 8 nm.

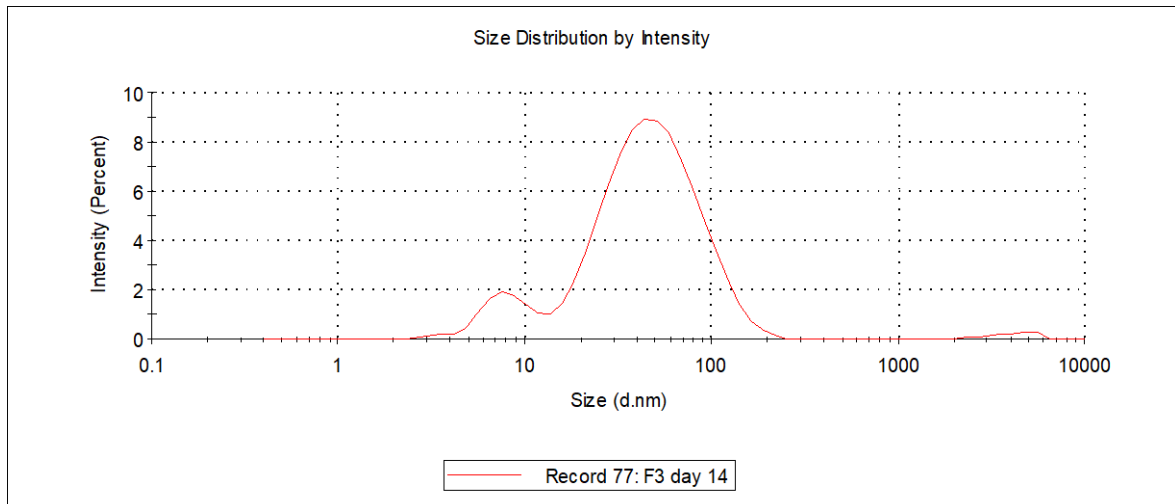


Figure 41: Graph showing particle size distribution in a sample containing 0,01% CsA after 14 days of incubation at 5-6°C.

In some samples, we have also observed some intensity produced by very big particles. We are assuming that this was the dust in the cuvette, as the intensity of this peak was always really low (max. 2.0%).

If we observe the size of the peak 1 (around 50 nm) through time, we see that it is stable and that it does not change till the end of the stability test. Only one big fall was detected after the first week and this was probably a consequence of our system getting into the most stable phase following the manufacture of eye drops (Figures 42, 43 and 44).

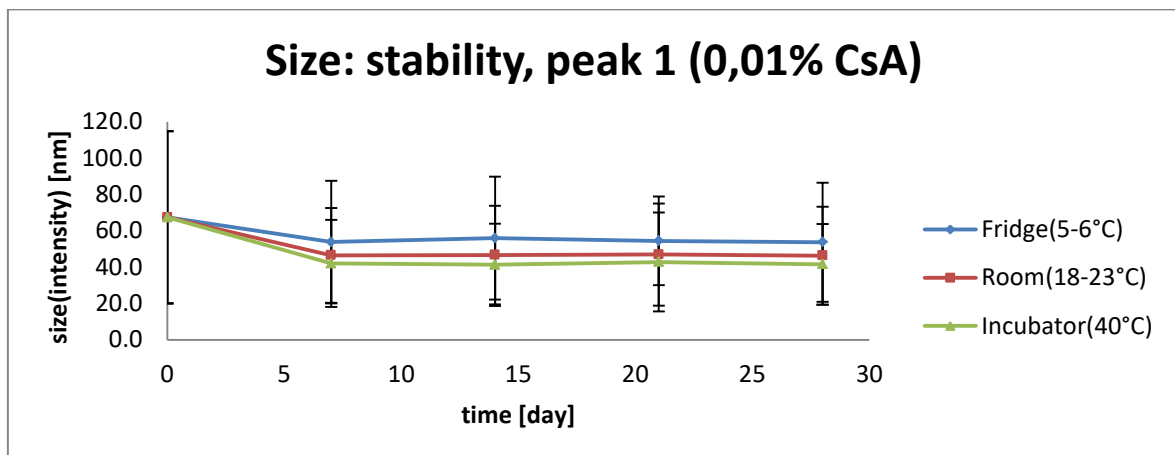


Figure 42: Graphical presentation of peak 1 particle size changes (intensities) in formulations containing 0,01% CsA during the stability study, carried out at different conditions.

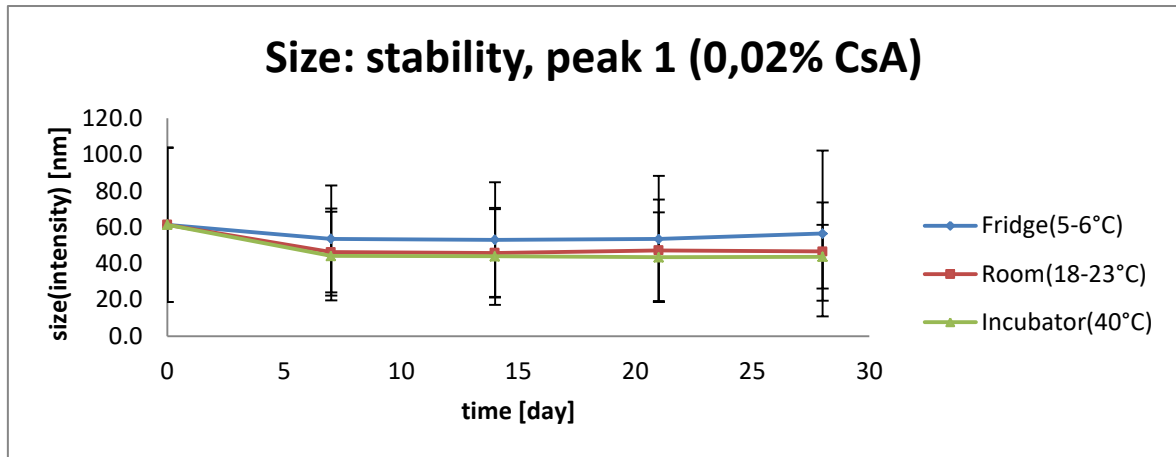


Figure 43: Graphical presentation of peak 1 particle size changes (intensities) in formulations containing 0,02% CsA during the stability study, carried out at different conditions.

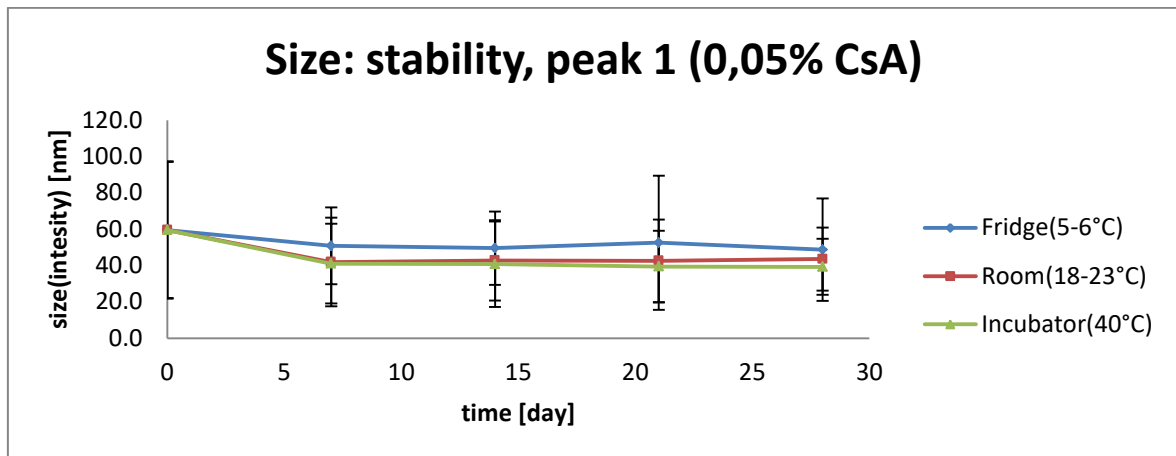


Figure 44: Graphical presentation of peak 1 particle size changes (intensities) in formulations containing 0,05% CsA during the stability study, carried out at different conditions.

Furthermore, when we compared the intensities of peaks 1 and 2, they did not change over time. We could not reach 100% intensity because of the presence of some bigger particle populations within the formulation. These were probably dust or possibly coagulated dispersion particles.

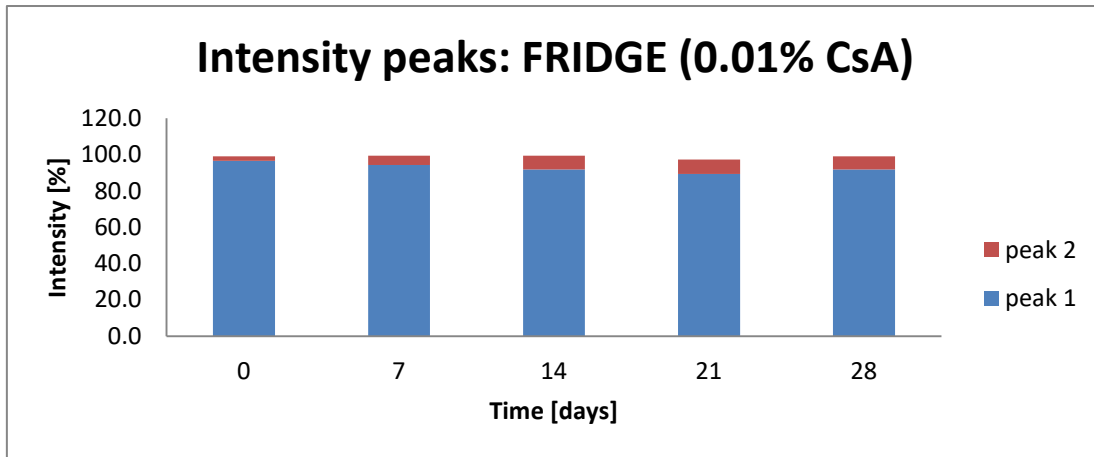


Figure 45: Stacked bar graphs showing the percentages of intensities of two peaks present within the particle population in formulations containing 0.01% CsA that were kept in fridge at 5 – 6 °C, for 28 days.

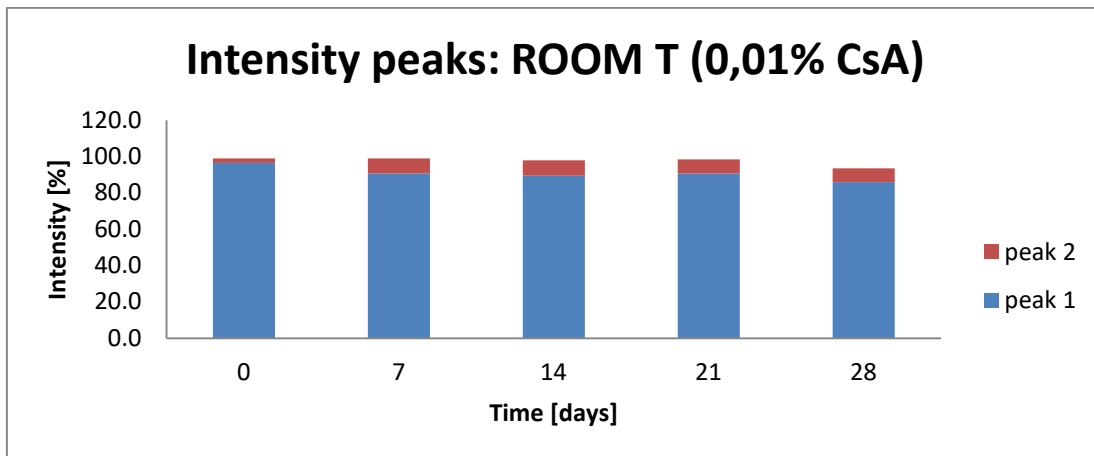


Figure 46: Stacked bar graphs showing the percentages of intensities of two peaks present within the particle population in formulations containing 0.01% CsA that were kept in fridge at room temperature (18 – 23 °C), for 28 days.

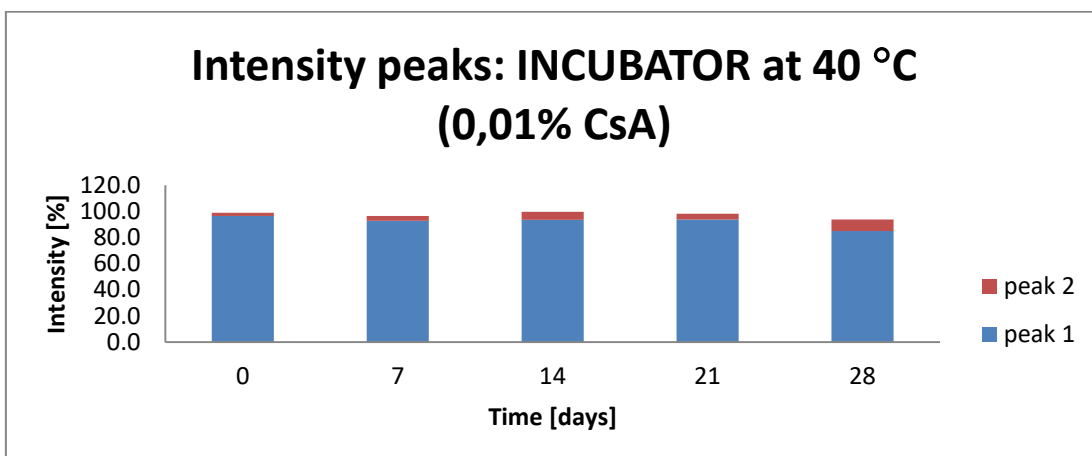


Figure 47: Stacked bar graphs showing the percentages of intensities of two peaks present within the particle population in formulations containing 0.01% CsA that were kept in incubator at 40 °C, for 28 days.

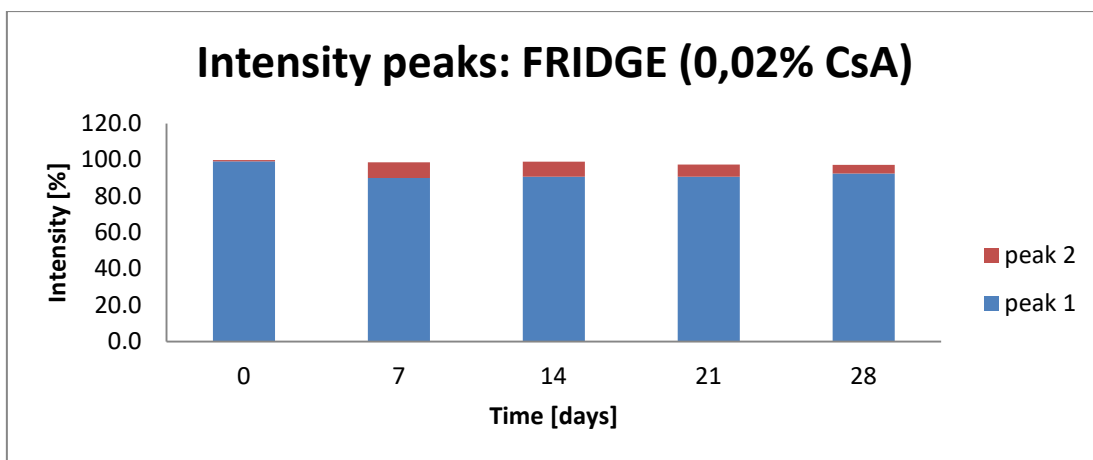


Figure 48: Stacked bar graphs showing the percentages of intensities of two peaks present within the particle population in formulations containing 0.02% CsA that were kept in fridge at 5 – 6 °C, for 28 days.

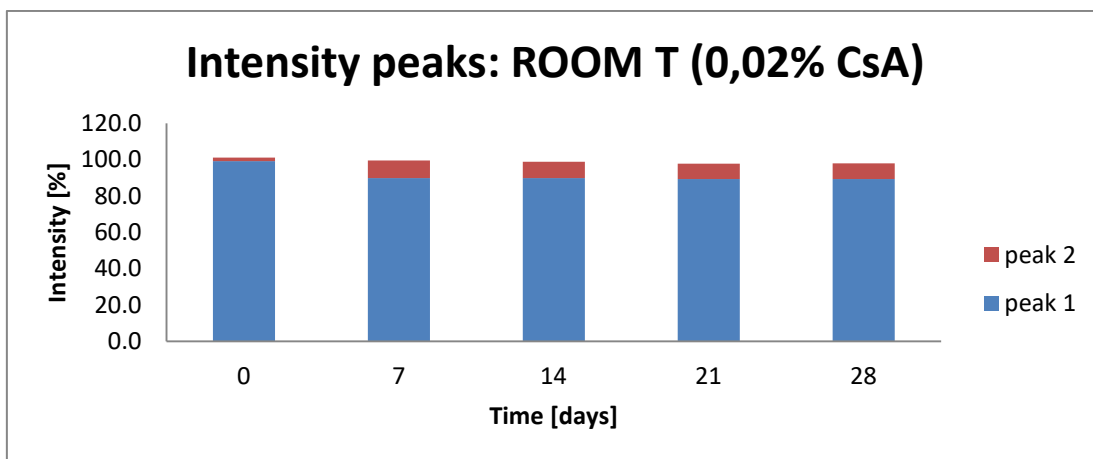


Figure 49: Stacked bar graphs showing the percentages of intensities of two peaks present within the particle population in formulations containing 0.02% CsA that were kept in fridge at room temperature (18 – 23 °C), for 28 days.

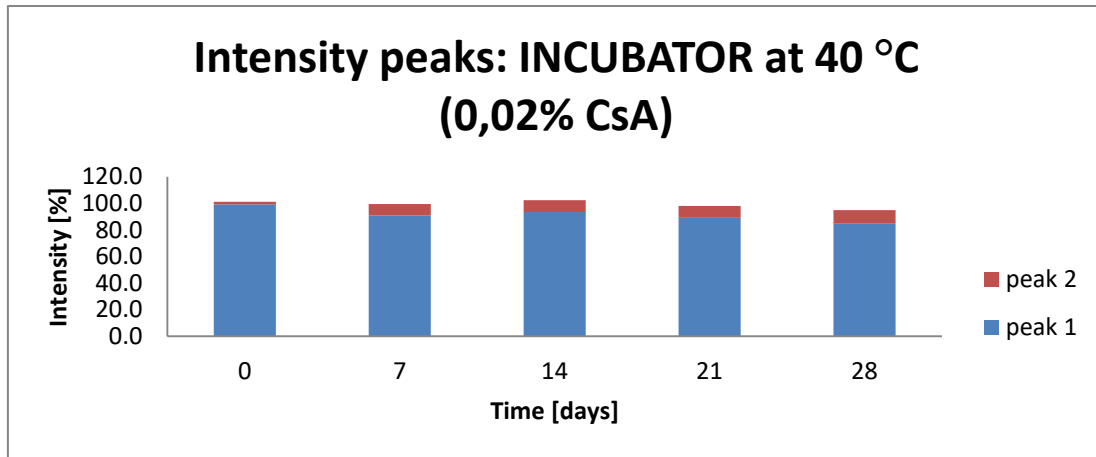


Figure 50: Stacked bar graphs showing the percentages of intensities of two peaks present within the particle population in formulations containing 0.02% CsA that were kept in incubator at 40 °C, for 28 days.

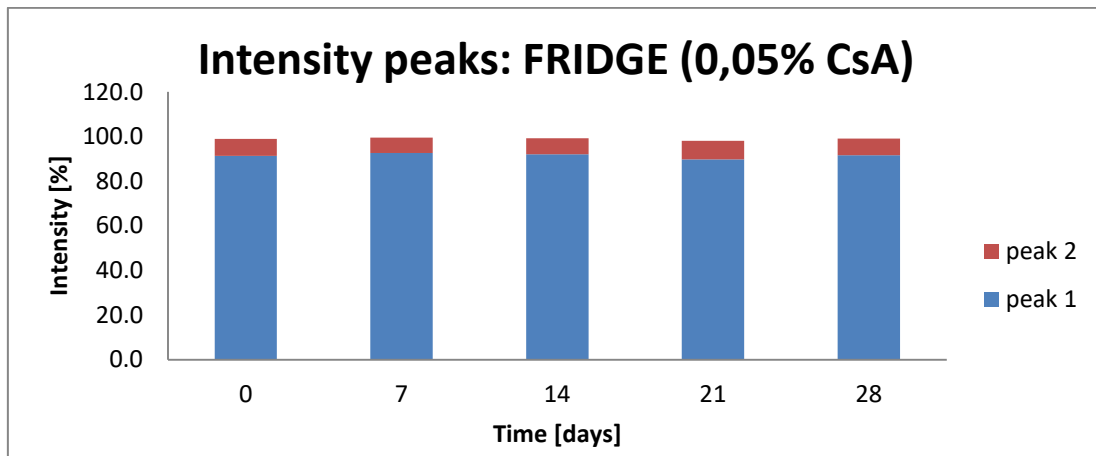


Figure 51: Stacked bar graphs showing the percentages of intensities of two peaks present within the particle population in formulations containing 0.05% CsA that were kept in fridge at 5 – 6 °C, for 28 days.

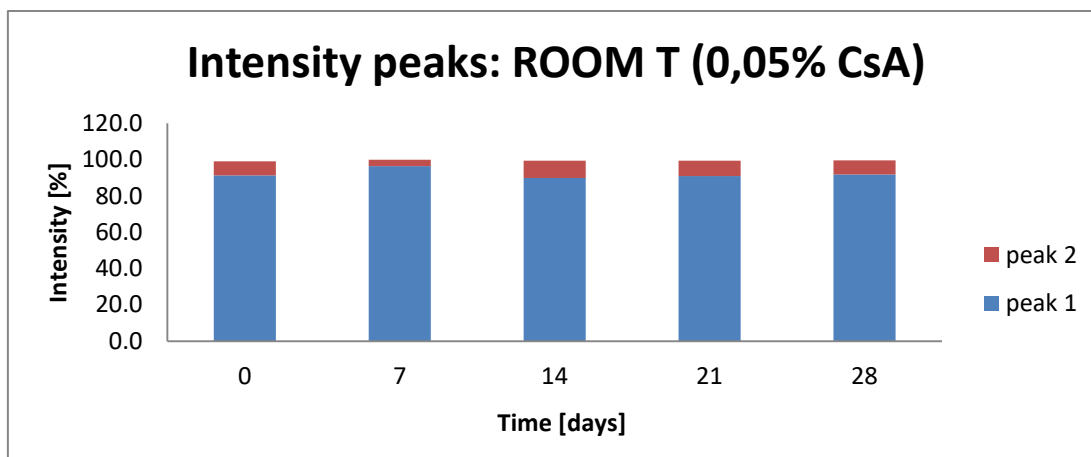


Figure 52: Stacked bar graphs showing the percentages of intensities of two peaks present within the particle population in formulations containing 0.05% CsA that were kept in fridge at room temperature (18 – 23 °C), for 28 days.

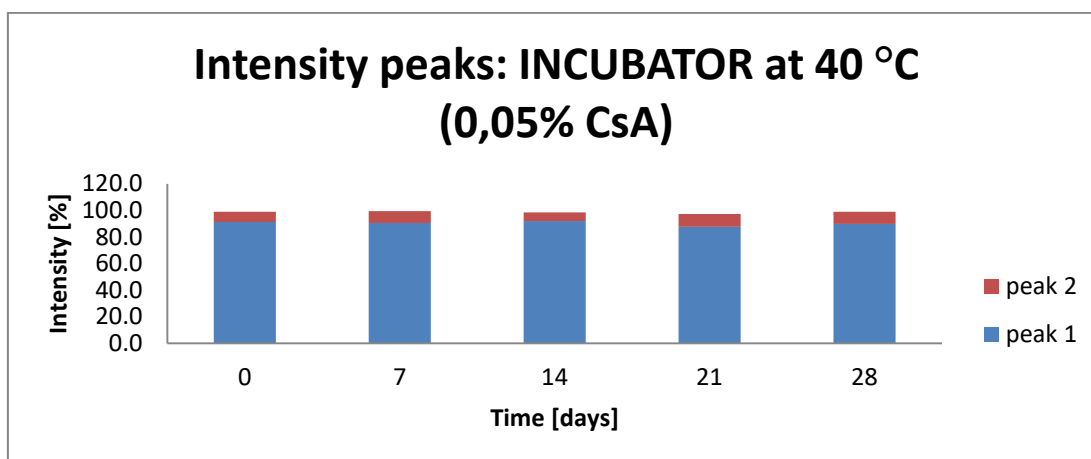


Figure 53: Stacked bar graphs showing the percentages of intensities of two peaks present within the particle population in formulations containing 0.02% CsA that were kept in incubator at 40 °C, for 28 days.

In addition to particle size peak data we have also looked at the poly-dispersity indices (PDI) for all formulations tested at different times at different temperatures (Figures 54, 55 and 56).

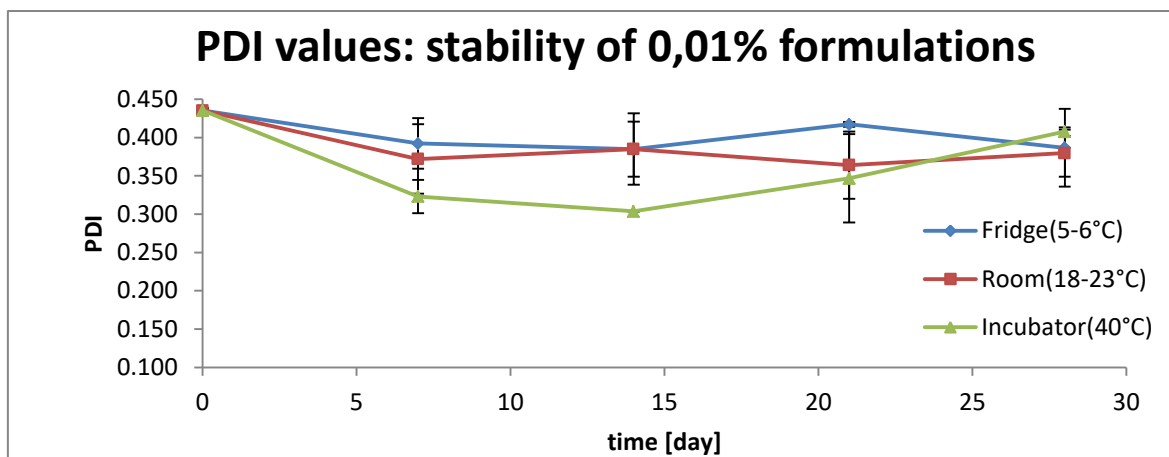


Figure 54: Graphical presentation of poly-dispersity index changes (PDI) in formulations containing 0.01% CsA during the course of the 28 days long stability study, carried out at different conditions.

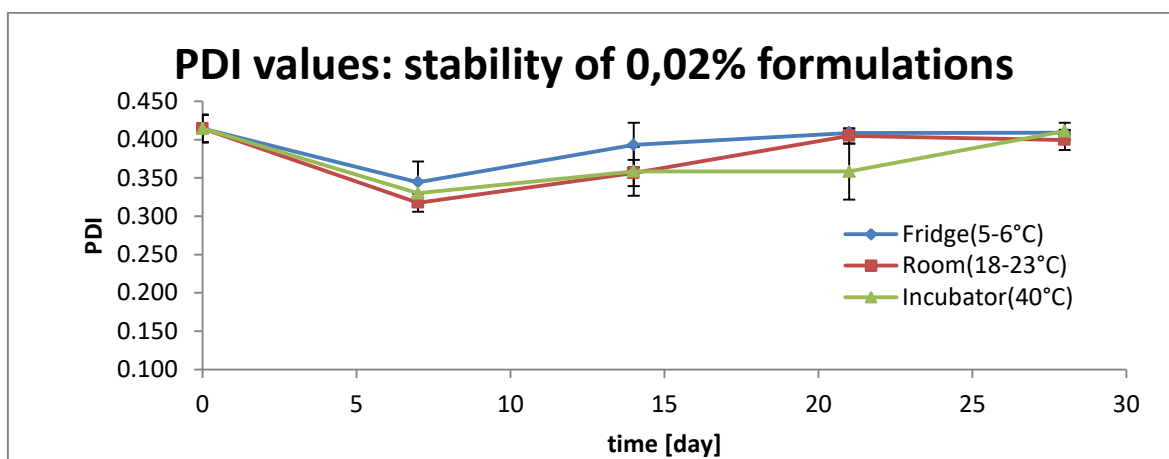


Figure 55: Graphical presentation of poly-dispersity index changes (PDI) in formulations containing 0.02% CsA during the course of the 28 days long stability study, carried out at different conditions.

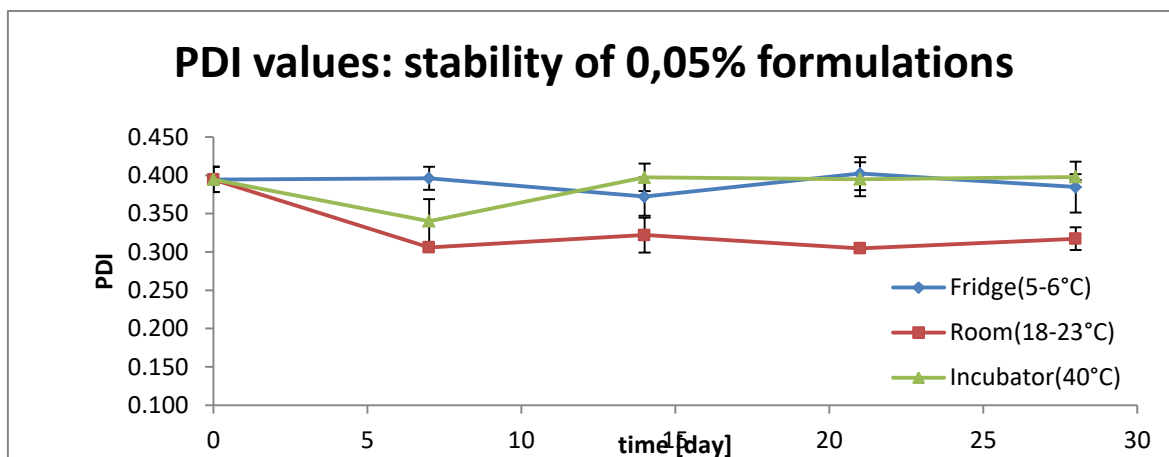


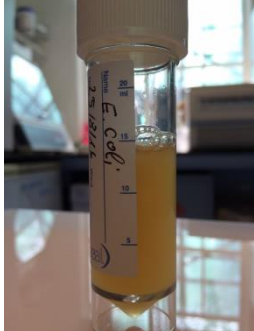
Figure 56: Graphical presentation of poly-dispersity index changes (PDI) in formulations containing 0.05% CsA during the course of the 28 days long stability study, carried out at different conditions.

PDI values show us how wide the particle distribution is. The higher the number, the less monodispersed are the nanoparticles. Furthermore, if we compare PDI values over the time course of the stability study (Figures 54, 55 and 56) we see that they stay more or less the same, meaning that the particles did not form any bigger aggregates or clumps. Still we can see some small PDI value rises at certain time points. The reason for that is the already mentioned third peak within the population, which is probably due to a presence of bigger impurity particles, such as dust.

#### 4.7. Sterility test, according to USP 39

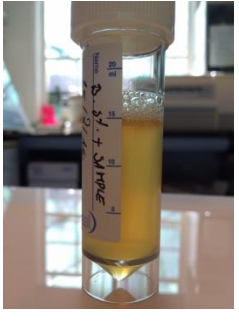
In production of eye drops we have to assure that the final product in packed in container is sterile. We used sterile filtration through 0.22  $\mu\text{m}$  syringe membrane filters as the sterilization process carried out in aseptic conditions. Sterility of our formulations was tested on the samples, taken from three containers, according to the United States Pharmacopeia 39 (USP). However, as we could not provide all prescribed microorganisms for method suitability testing, we had to make some adjustments to the test.

#### 4.7.1. Growth promotion test

Sample	Presence of colony forming units (CFUs)	Tube photography
<i>S. aureus</i>	Yes	
<i>P. aeruginosa</i>	Yes	
<i>B. subtilis</i>	Yes	
<i>E. Coli</i>	Yes	

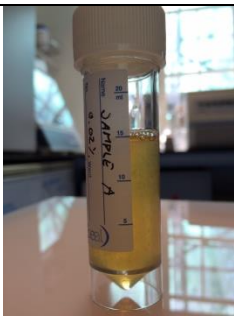
In growth promotion test we were testing the growth of bacteria in liquid TSB at 37°C. Tubes were incubated for 3 days.

#### 4.7.2. Method suitability test

Sample	Presence of CFUs	Tube photography
NM0133 + <i>S. aureus</i>	Not determined, due to turbidity, see Table VIII	
NM0133 + <i>P. aeruginosa</i>	Not determined, due to turbidity, see Table VIII	
NM0133 + <i>B. subtilis</i>	Not determined, due to turbidity, see Table VIII	
NM0133 + <i>E. Coli</i>	Not determined, due to turbidity, see Table VIII	

In method suitability test we were testing the growth of bacteria in liquid TSB in presence of our formulation at 37°C. Tubes were incubated for 3 days.

### 4.7.3. Sterility test

Sample	Presence of CFUs	Tube photography
NM0133 A	Not determined, due to turbidity, see Table VIII	
NM0133 B	Not determined, due to turbidity, see Table VIII	
NM0133 C	Not determined, due to turbidity, see Table VIII	
Negative control with sterile water	No	
Negative control without sterile water	No	

#### 4.7.4. Plates

Because in 50 mL centrifuge tubes containing TSB it was impossible to determine if there was any bacterial growth, we have inoculated the plates as described in the methods section.

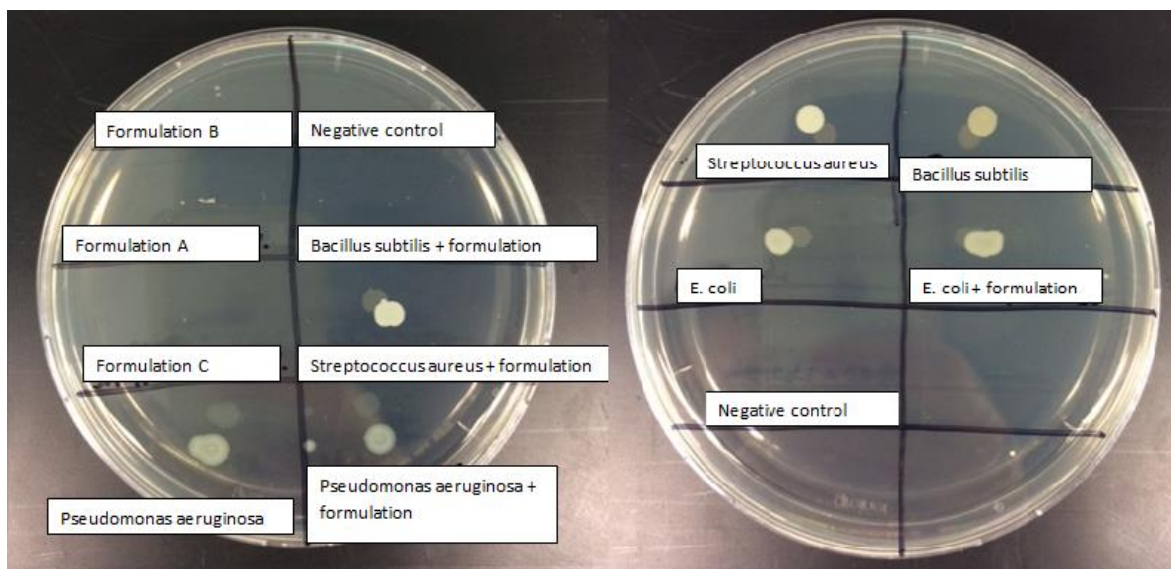


Figure 57: Photography showing Petri dishes with TSB agar inoculated with bacteria, samples of our formulations and negative controls. For detailed explanation, please see Table VIII.

Table VIII: Bacterial growth on agar plates.

Sample name	Presence of growth
<i>S. aureus</i>	Yes
<i>P. aeruginosa</i>	Yes
<i>B. subtilis</i>	Yes
<i>E. Coli</i>	Yes
Formulation mixed + <i>S. aureus</i>	Yes
Formulation mixed + <i>P. aeruginosa</i>	Yes
Formulation mixed + <i>B. subtilis</i>	No
Formulation mixed + <i>E. Coli</i>	Yes
Formulation A	No

Formulation B	No
Formulation C	No
Negative control	No
Negative control	No

In the growth promotion test the microorganisms were tested in defined broth (TSB) for their growth. As seen from results (Figure 57 and Table VIII) all four microorganisms used in test grew. In the method suitability test a small amounts of bacteria were added into tubes containing TSB, together with samples of our formulation. In this way the impacts of samples on the growth of each bacteria was tested. We observed that our formulation only interfered with *B. subtilis* where no growth of bacteria was found. The three samples (A, B and C) of our formulations, as well as negative controls alone, produced no bacterial growth, a result indicating sterile product.

## 5. Conclusion

The main part of our master thesis was a one month long stability test of eye drops formulations, containing GCPQ nanoparticles and three different encapsulated concentrations of cyclosporine A (CsA). First we synthesised the GCPQ polymer and used it (in a concentration of 0,75%) for production of our formulations, containing 0,01%, 0,02% and 0,05% CSA. The whole procedure of eye drops production was optimized and additionally, the sterility test of formulations, according to USP 39 was carried out.

Our data show, that 10 - 15 cycles of homogenization were enough to achieve desired particle sizes, and that keeping the formulations at low temperature environment (fridge) while stirring, before homogenization, increased the solubility of CsA in water. We have also showed that reduced numbers of homogenisation cycles do not impact the stability of eye drops.

The stability test data confirm that our formulations were stable over 28 days, when kept in fridge (5 – 6 °C), at room temperature (18 – 23 °C) or in incubator (40 °C), as no major changes in their characteristic were observed under these conditions. We think that all small differences in stability study data were the results of human error, evaporation of water from formulations kept in plastic bottles and dust being present in samples during the measurements of dispersed GCPQ polymer particle sizes.

We also carried out the sterility test according to the USP 39 in order to prove that the sterilization process (filtration) of eye drops was successful. Unfortunately not all of the prescribed microorganisms were available, however with those that were used, all tested formulations have passed the test.

## 6. Literature

1. New poll: Americans fear blindness more than loss of other senses, strongly support more funding for research [Internet]. Association for Research and Vision in Ophthalmology (ARVO).  
[http://arvo.org/About\\_ARVO/Press\\_Room/New\\_poll\\_\\_Americans\\_fear\\_blindness\\_more\\_than\\_loss\\_of\\_other\\_senses,\\_strongly\\_support\\_more\\_funding\\_for\\_research/](http://arvo.org/About_ARVO/Press_Room/New_poll__Americans_fear_blindness_more_than_loss_of_other_senses,_strongly_support_more_funding_for_research/)
2. Visual impairment and blindness;  
<http://www.who.int/mediacentre/factsheets/fs282/en/>
3. Drake R, Vogl AW, Mitchell AWM. Gray's anatomy for students. 2nd ed. Philadelphia; 2010.
4. Saladin KS. Anatomy & physiology : the unity of form and function. 6th ed. New York, London; 2011.
5. Kruse FE, Cursiefen C, Seitz B, Völcker HE, Naumann GOH, Holbach L. Klassifikation der Erkrankungen der Augenoberfläche. Der Ophthalmol [Internet]. 2003;100(11):899–916. Available from: <http://link.springer.com/10.1007/s00347-003-0937-5>
6. <http://www.ncbi.nlm.nih.gov/pubmed/24150468>\n<http://www.pubmedcentral.nih.gov/articlerender.fcgi?artid=PMC4049531>
7. Smith AF, Waycaster C. Estimate of the direct and indirect annual cost of bacterial conjunctivitis in the United States. 2009;11:1–11.
8. Ibrahim YW, Boase DL, Cree IA. Incidence of Infectious Corneal Ulcers , Portsmouth Study , UK. 2012;1–4.
9. Jeng BH, Gritz DC, Kumar AB, Holsclaw DS, Porco TC, Smith SD, et al. Epidemiology of ulcerative keratitis in Northern California. Arch Ophthalmol. 2010;128(8):1022–8.
10. Gayton JL. Etiology, prevalence, and treatment of dry eye disease. Clin Ophthalmol (Auckland, NZ). 2009;3:405.

11. Tasman W, Jaeger EA. The Wills Eye Hospital atlas of clinical ophthalmology. 2nd ed. Philadelphia: Lippincott Williams & Wilkins;
12. Quigley HA, Vitale S. Models of open-angle glaucoma prevalence and incidence in the United States. *Investig Ophthalmol Vis Sci.* 1997;38(1):83–91.
13. Honik G, Wong IG, Gritz DC. Incidence and Prevalence of Episcleritis and Scleritis in Northern California. *Cornea.* 2013;32(12):1562–6.
14. Mitra AK. Ophthalmic drug delivery systems. New York: Marcel Dekker Inc; 2003.
15. Florence AT, J S. Modern pharmaceuticals. 5th ed. New York, London: Informa Healthcare; 2009.
16. Patel A, Cholkar K, Agrahari V, Mitra AK. Ocular drug delivery systems: An overview. 2015;2(2):47–64.
17. Dhankhar P. Homogenization Fundamentals. 2014;04(05):1–8.
18. <https://www.youtube.com/watch?v=UpvIQwRYe-E>
19. Qu X, Khutoryanskiy V V, Stewart A, Rahman S, Papahadjopoulos-sternberg B, Dufes C, et al. Carbohydrate-Based Micelle Clusters Which Enhance Hydrophobic Drug Bioavailability by Up to 1 Order of Magnitude. 2006;3452–9.
20. Soundararajan R, Gaisford S, Arifin N, Chooi KARWAI, Isabel M, Ao SIM. Physical Characterisation and Long-Term Stability Studies on Quaternary Ammonium Palmitoyl Glycol Chitosan ( GCPQ )— A. 2014;2296–306.
21. Uchegbu IF, Sadiq L, Arastoo M, Gray AI, Wang W, Waigh RD, et al. Quaternary ammonium palmitoyl glycol chitosan — a new polysoap for drug delivery. 2001;224:185–99.
22. Uchegbu IF. Delivery of Peptides to the Blood and Brain after Oral Uptake of Quaternary Ammonium Palmitoyl Glycol Chitosan Nanoparticles. 2012;
23. Siew A, Le H, Thiovolet M, Gellert P, Schatzlein A, Uchegbu I. Enhanced Oral Absorption of Hydrophobic and Hydrophilic Drugs Using Quaternary Ammonium Palmitoyl Glycol Chitosan Nanoparticles. *Mol Pharm.* 2012;9:14–28.

24. Matsuda S, Koyasu S. Mechanisms of action of cyclosporine. 2000;119–25.
25. No Title [Internet]. Available from:  
<https://de.wikipedia.org/wiki/Ciclosporin#/media/File:Ciclosporin.svg>
26. Sartor M. Dynamic light scattering. University of California San Diego;
27. Instruments M. INFORM WHITE PAPER DYNAMIC LIGHT SCATTERING. 2011.
28. Goldberg WI, Introduction I. Dynamic light scattering. 1999;(May):1152–60.
29. Dynamics C. The Zeta Potential. Sydney: Colloidal Dynamics Inc; 1999. p. 1–4.
30. <http://www.lenntech.de/zetapotential-de.htm>
31. <http://www.learningace.com/doc/2946038/fd53fbdf18aa5d00684292556af93695/zetasizer-chapter-16>
32. <http://medical-dictionary.thefreedictionary.com/osmolarity>
33. <http://www.loeser-osmometer.de/osmometrie-eng.html>
34. <http://physics.info/viscosity/>
35. Technologies Inc A. Agilent 1290 Infinity Evaporative Light Scattering Detector ( ELSD ). Agilent Technologies; 2012.
36. Bedford N. Principles of Operation of an Evaporative Light-Scattering Detector for Liquid Chromatography. 1984;2427–34.
37. Ismailos G, Reppas C, B. Dressaman J, Macheras P. Unusual solubility behaviour of cyclosporine A in aqueous media. J Pharm Pharmacol. 1991;43(4):287–9.
38. Avestin C5 homogenizator; <http://www.aveston.com/Images08/c5pic2.jpg>
39. Soundararajan R, Gaisford S, Arifin N, Chooi KARWAI, Isabel M, Ao SIM. Physical Characterisation and Long-Term Stability Studies on Quaternary Ammonium Palmitoyl Glycol Chitosan ( GCPQ )— A. Willey Online Libr. 2014;2296–306.